Color image technique in fish research

Yevgeniya Shatilova

Master's thesis
Department of Computer Science
University of Joensuu

Color image technique in fish research

Yevgeniya Shatilova

Department of Computer Science and Statistics
P.O. Box 111, FI-80101 Joensuu, FINLAND.

Master's thesis
February, 2008

Abstract

The aim of this work is to study and apply color technique for non-destructive approximation of the carotenoids amount in fish skin. The object of the study is Arctic charr (*Salvelinus alpinus*) and its carotenoids-based coloration.

For this purpose an affordable method for assessing carotenoids content in fish skin based on digital imaging reconstructed into spectral reflectance was proposed and examined. A polynomial regression method was investigated to improve the accuracy of the reconstruction of fish spectra. A polynomial model and an extended training set enhanced spectral reconstruction were determined. The correlation between carotenoids concentration in fish skin and their spectral reflectance was examined; results confirmed a feasibility of the proposed method. The technique allows to avoid an expensive and long chemical analysis required a sacrificing of fish specimens.

The research work was performed in co-operation with Biology Department of University of Joensuu for their purposes.

Keywords: spectral reconstruction, spectral imaging, carotenoids, Arctic charr

Acknowledgements

I would like to sincerely thank people who supported me during my studies and especially during my research work. I would like to express my sincere appreciation and my gratitude to Professor Jussi Parkkinen, Dean of the Faculty of Science at the University of Joensuu, for the opportunity to participate in IMPIT program and Color Research Group.

I would like to thank to my supervisor Birgitta Martinkauppi for her guidance, patience and real help that could not be overestimated. I would like to express my gratitude to Jukka Kekäläinen for his help and interesting collaboration work.

I would like to thank people from Color research group of the University of Joensuu. Particularly, I want to express my thanks to Vladimir Bochko who was always ready to help to solve any challenges and discuss on any topics.

I want to thanks all my friends and my dear Yasser for support and inspiration.

And finally, I would like to express my deepest appreciation and thanks to my family. Thank you for their support, help and believe in my ability.

CONTENTS

1. INTRODUCTION

1.1. Overview

Color as a property may give us the knowledge about an object. In biological science, a variety of colors may convey valuable information. Any color changes in plants or animals may provide significant information about their state which then can be studied and interpreted by scientists. The coloration of animals is produced with different color pigments. Recently, the evolutionary biologists have interested in identifying in carotenoids-derived nature of fish coloration. Knowledge about the types and content of color pigment is important in social and sexual contexts [McGraw et al., 2005].

In present day, colors and their digital representations are becoming of increasing importance in every day life. The possibilities to measure color's characteristics of an object by using the modern imaging systems facilitate the investigation the color properties of an object and open a wide range of opportunity to scientists in their research works. High computational resources and systems for digital image processing are becoming more popular in various industry fields such as medicine, biology, forestry etc.

This research focuses on the study of color and its characteristics in biological areas, namely in fish research. The ***object*** of this study is a species of fish called *Arctic charr* (*Salvelinus alpinus*) (Fig. 1.1). Arctic charr is considered an endangered species in Finland and studied by the biology scientists to restore this population of fish. A red coloration of this fish is carotenoids-based coloration. It is assumed to be a factor defining the sexual behavior of fish during spawning period. The high level of carotenoids in fish skin may be indicator on male attractiveness, activity and ability to produce health posterity [Lozano, 1994; Grether et al., 2004]. Knowledge about carotenoids content is critical in biological research for determination health state, social and sexual contexts of fish. The relationships between carotenoids in the integument, level of immune-system function and sexual attractiveness were tested and a positive correlation has been revealed [Grether et al., 2004].

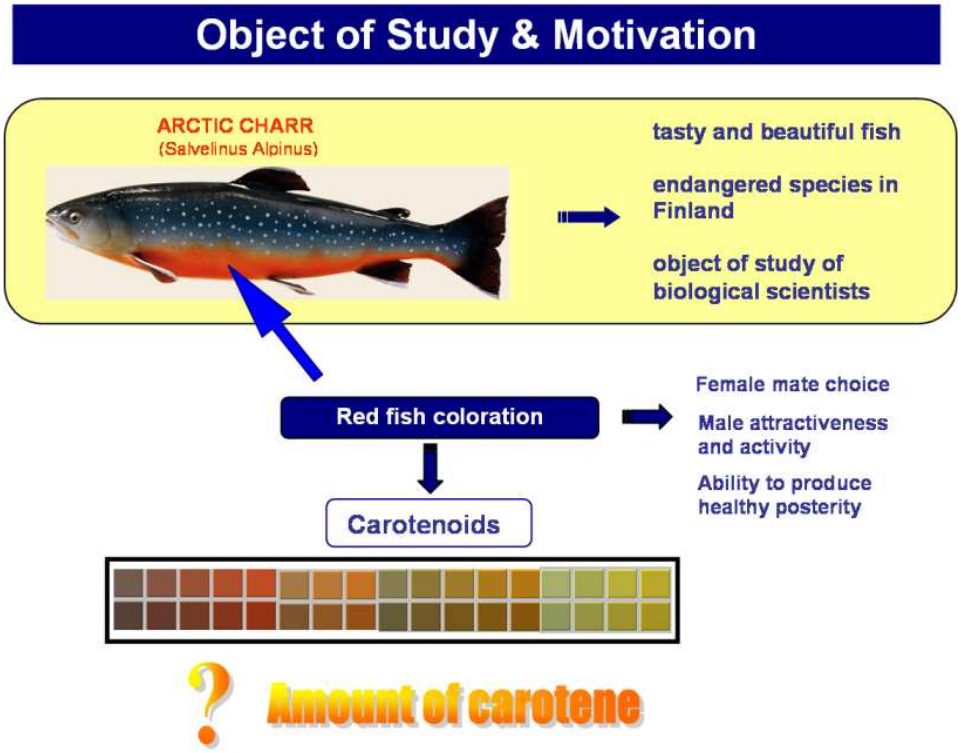

Figure 1.1: Arctic charr as an object of the study

This thesis has been carried out in co-operation with Biology Department of University of Joensuu. In this work, obtained knowledge about studied fish species were combined and reinvestigated from two points of view - biology and color science – in order to get effective results in study of this species.

1.2. Study objectives

As described, assessing carotenoids content is important for determination valuable information about different characteristics of fish individual. Carotenoids can be extracted and quantified with complex chemical analysis which is expensive.

The main ***objective*** of this study was to develop and test affordable method for determination of an approximation of carotenoids amount of Arctic charr which can facilitate the conduction of the biological research of this fish. Due to all the limitations of fish research (see next section), an algorithm shown in Fig. 1.2 was proposed to approximation the carotenoids amount in Acrtic charr's skin based on RGB image.

Figure 1.2: Algorithm for approximation amount of carotenoids in fish skin

To achieve the objective following research goals were established:

- To study spectral reconstruction method based on digital camera responses and adopt to fish images
- To acquire and analyze the spectral images of fish skin with different intensity of carotenoids-based coloration
- To examine the correlation mechanism between the measured carotenoids concentration in fish skin and corresponding reflectance spectra
- To find out whether the correlation can provide significant prediction of carotenoids quantity in fish skin based on spectra information

1.3. Scope, limitations, and constraints

Fish research imposes definite constraints and limitations. Let us to outline the main ones. Ideally, spectral reflectance of fish which provides accurate color's information (see section 3.3) would probably be the most convenient metric to estimate the color pigment amount in fish skin.

The major drawback of this study is the acquisition of the spectral images of fish. First of all, taking spectra of fish involves the sacrifice of fish which should be avoided in light of conservation of this species. Moreover, the spectra acquisition of fish takes long time which can have a negative effect in respect to changes of fish coloration. From another point of view, spectral imaging devices require certain experience and special skills to use. In addition, such devices are expensive and not portable. Other limitations are constant and intense light source which has to be applied directly to the flattened and size-fixed sample area. This mode creates difficulties with imaging of flashy parts such as fish skin.

In an attempt to overcome the difficulties and limitations in spectral imaging, the spectral reconstruction method from digital camera responses was utilized [see section 3.4]. The taking of RGB images is the most appropriate approach in case of fish research. But using RGB values from a digital device for estimation can not guarantee precise solutions, since the trichromatic technique does not provide the accurate color quality. The main limitations of digital color representation and corresponding spectra reconstruction are light- and device-dependencies. Moreover performance of spectra estimation from camera responses depends on camera [8].

1.4. Thesis organization

This thesis is arranged as follows. Chapter 2 provides a detailed description about the main object of this study. Readers can obtain common information about fish species such as *Arctic charr* and an introduction to the carotenoids color pigment. In this chapter an uncommon field of study for color experts is presented which describes the essential motivation to research.

Chapter 3 describes an introduction to light and color and presents the basic color imaging technique and methods used to investigate the object of this study.

Chapter 4 provides a description of the testing of spectral reconstruction based on polynomial regression method. Testing was done by using 2^{nd} and 3^{rd} order of polynomial and different training set. As a result of the chapter, the best type of polynomial function and extended selected training set has been chosen.

Chapter 5 presents the results obtained during spectral measurements of fish skin. The Chapter contains the processing the outcomes of the examination of the correlation between carotenoids amount in skin and their spectra.

All work summarized in Chapter 6. Discussion and conclusions of this study are presented with possible suggestion of improvement.

2. ARCTIC CHARR AND COLOR

2.1. Overview

The object of this study is a fish species named *Arctic charr*. Let us take a close look at this mysterious fish which has triggered our rapt attention.

Generally, Arctic charr (*Salvelinus alpinus*) is related to the Salmonidae family, native to Arctic, sub-Arctic and alpine lakes and coastal waters. This species can be regarded as the northernmost freshwater fish in the world.

Arctic charr is possibly the oldest and the most beautiful freshwater fish living in Finland [Arctic Centre, Karttaikkuna Oy]. Northern Lapland is the main part of charr's location especially in the municipalities of Utsjoki, Inari and Enontekiö. In Lapland, Arctic charr is often called "Rautu", the small one is called "Paltsarautu" and "Nieriä" in North Karelia [Arctic Centre].

The tasty meat of the Arctic charr attracts people to breed this species. That is why many attempts have been made to breed and introduce it to suitable conditions. This fish species is very sensitive to environmental changes and this makes breeding quite difficult. Additionally, breeding meet other problems like net fishing and competition since Arctic charr is a week competitor and the population can be injured by other species [Karttaikkuna Oy].

The coloration of the charr is wonderful in autumn during the spawning season. In this period the males commonly develop a deep red color in their abdomen [Karttaikkuna Oy]. Their carotenoids-based coloration becomes brighter with a dark back and bright red and orange underbelly (Fig. 2.1).

Figure 2.1: Arctic charr [Arctic Centre]

In Finland the Arctic charr is considered at risk of disappearing species. This fish can be alarmingly endangered because of the influence of threat factors such as the regulation of watercourses, excessive fishing and the eutrophication of waters. For instance, if to compare catches of Arctic charr nowadays with 1930s before regularization started, they are declining regularly [Karttaikkuna Oy].

Biology scientists are studying how to protect and restore the Arctic charr population. The crucial point to consider in increasing fish population is to enhance the amount of posterity. As such in the spawning season this should provide qualitative and quantitative descendants. There is a number of scientific works in which fish sexual selection has been discussed and the red coloration has been considered important in mate choice [Masvaer et al., 2004; Saks et al., 2003]. Masvaer *et al* concluded that "*females evaluating male abdominal coloration may obtain information about differences between males in fertilization potential*" [Masvaer et al., 2004]. The red coloration of fish can be considered as a factor defining behavior during mating period and its activity and ability to produce healthy posterity. Thus, fish redness can be regarded as an indicator of successful individuals.

From a biological point of view, the color pigment responsible for many of red, orange and yellow colors in nature is carotenoids pigments [Humphries et al., 2004; von Schantz et al., 1999]. Arctic charr is "*an excellent example of the species developing a strong carotenoid based coloration adjoining the spawning period*" [Martinkauppi et al., 2007].

2.2. Carotenoids as signals

Recently carotenoids pigments have become popular in the study of sexual selection in animals. Biological scientists argue that carotenoids play a major role in the mechanism of selection. The amount of carotenoids as a colorant for skin, scales is limited because animals can not produce carotenoids but acquire them from foods. The main assumption of most science studies is that carotenoids-based color accurately reflects the amount of carotenoids within pigment patch [Saks et al., 2003].

Color pigments such as carotenoids and melanins play important role in animal's coloration. Carotenoid pigments are responsible for red, orange and yellow colors, while melanin pigments produce colors from an achromatic black to brown. Thank to these color pigments different animals such as birds, fish, lizards, frogs, penguins and etc obtain various coloration depending on season time [Hofmann et al., 2007].

In biological terms, the pigment cells of multicellular organisms are called as chromatophores. Fish chromatophores can be characterized by different types of cells. Coloration is the most important function in chromatophores of aquatic animals such as fish. Besides their role in coloration of fish, the chromatophores play significant roles in temperature regulation and protection from harmful radiation [Sugimoto & Oshima, 2002].

According to Chatzifotis *et al.* [Chatzifotis et al., 2005] color of fish skin depends on the presence of chromatophores which can be classified into six types (melanophores, xanthophores, erythrophores, iridophores, leucophores and cyanophores). These chromatophores contain pigments such as melanins, carotenoids (e.g. astaxanthin, canthaxanthin, lutein and zeaxanthin), pteridines and purines. Color depends on the types and concentrations of carotenoid pigments present. A mixture of pigments provides the continuous variation from red to yellow distinguishing by the ratio of red to yellow carotenoids [Hofmann et al., 2006].

There are a number of works studied the relationship between coloration and color pigment. Saks *et al.* [Saks et al., 2003] considered the relationship between hue, chroma and brightness and caroteniod pigment content in feather of birds and found positive correlation. Earlier studies have shown the correlation in living plants; for example,

between spectra reflectance and vitality of cucumbers (*Cucumis Sativus*) [Aario et al., 2001], assessing carotenoids content in plant leaves with spectral reflectance [Gitelson et al., 2002]. Humphries *et al.* have found the strong positive correlation between CIELAB b* and carotene concentration [Humphries et al., 2004].

This research focused on astraxanthin since this color pigment was found as a defining red-color of Arctic charr skin [Scalia et al., 1989]. The goal this study is to examine the strength and direction of the correlation between carotenoids (astaxanthin) concentration in fish skin and their spectral reflectance.

3. COLOR AND IMAGING

3.1. Color as phenomenon

The enigma of color has caught the attention of many of the most talented scientists. The question about the nature of color has been attracting humans since antiquity and it has resulted in diverse definitions. Intellectuals such as Aristotle, Grimaldi, Newton, Young, Maxwell and others have contributed to the knowledge surround of this topic.

First of all, the phenomenon of color exists only through human vision i.e. the human ability to perceive color. We can see things around us every day due to light, which can be natural or artificial. Sun light is the most important natural source for human and all living beings. Theoretically, light is a part of electromagnetic radiation that is visible to the average human eye [Field, 2004]. Visible colors are in the range between approximately 380 and 780 nanometers (nm) on the electromagnetic spectrum, as shown in Fig. 3.1.

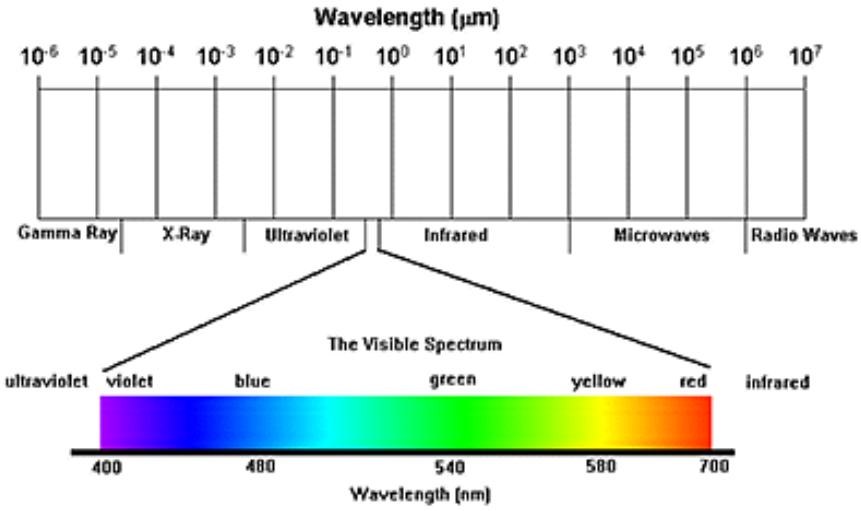

Figure 3.1: The visible spectrum as a part of electromagnetic radiation (adopted from http://www.daviddarling.info/encyclopedia/V/visible_light.html)

The various colors of objects are derived from the interaction between three participants: a light source, an object, and a detection system. The detection system can be artificial, human (observer) and another biological form. In human vision, color events occur as a sensations in the observer, originated by the spectrum of the light source and modified by

the colored object [Fraser et al., 2003] (Fig. 3.2). Colored surfaces transmit and reflect different amounts of wavelengths. If any component changes from this interaction, the color event may be different.

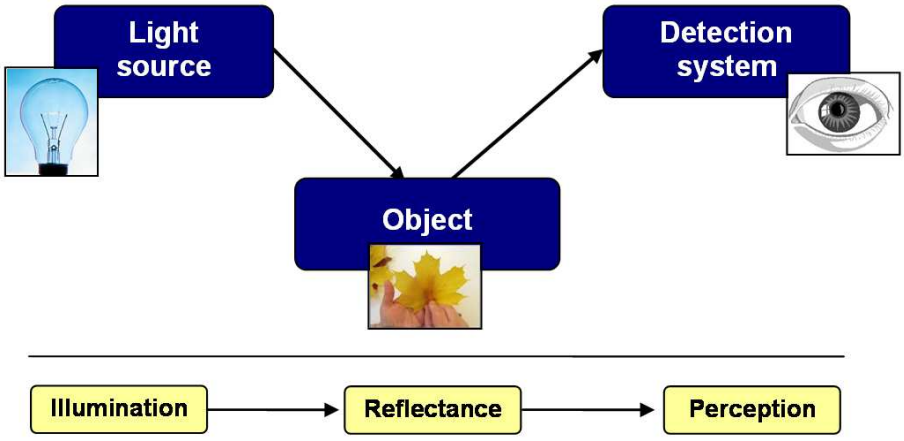

Figure 3.2: Color event as interaction between three participants

The CIE (Commission Internationale de l'Eclairage) or International Commission has specified a number of CIE Standard Illuminants. The term illuminant refers to "a light source that has been measured or specified formally in terms of spectral energy" [Fraser et al., 2003]. All the illuminants differ in their color temperature and spectral power distribution, i.e. power of light at each wavelength. Color temperature of the illuminant is the temperature at which a heated theoretical "black body" source produces light of the same visual color as the illuminant. There are a number of the most popular CIE illuminants [Fraser et al., 2003]:

- Illuminant A represents a tungsten light source with color temperature of 2856 K.
- Illuminant D is used to represent various model of daylight. The most commonly used are D50 and D65 (Fig. 3.3) with correlated color temperature of 5000K and 6504K, respectively.
- Illuminants F is a set of various types of fluorescent light source named F2, F3, and so on, up to F12.

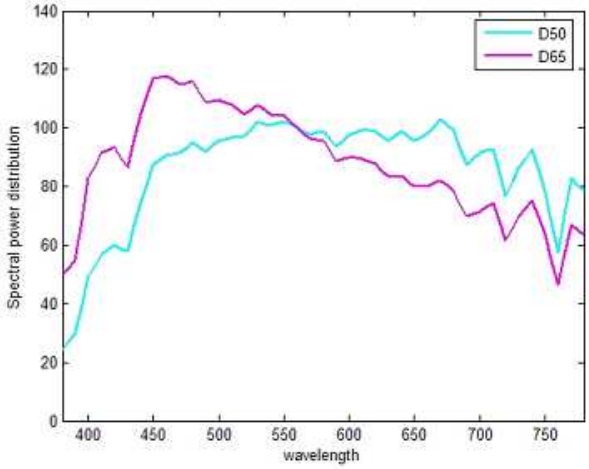

Figure 3.3: CIE Standard Illuminants D50 (blue) and D65 (red)

In this study, all the spectral measurements and digital imaging were done with D65 CIE Standard Illuminant.

The modified signal of light reflected from an object is perceived by an observer. The standard person can distinguish color based on wavelength of reflected or emitted light due to the structure of trichromatic human color vision proposed by Thomas Young (1802). According to this model, the human perception of color is achieved through three types of color receptors (cone) which are maximally sensitive to short, medium and long wavelengths of lights (S-, M- and L-cones), respectively (Fig. 3.4).

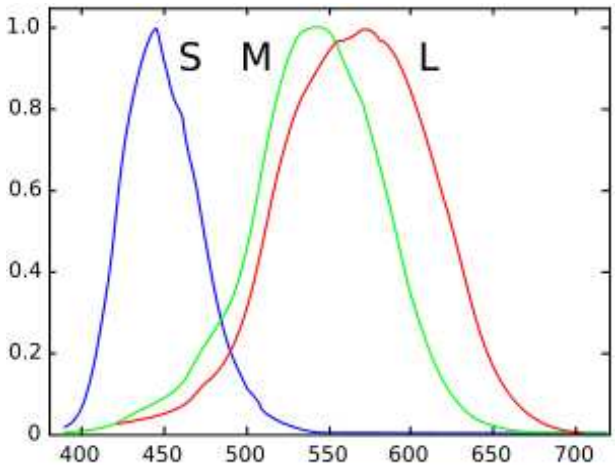

Figure 3.4: Cones absorption of light (adopted from http://en.wikipedia.org/wiki/Color_vision)

3.2. RGB and HSV as digital representation of color

Many ways have been suggested and different color models used for modeling and representing colors. The RGB color space is widely used in digital devices for capturing images and displaying them such as Charge-Coupled Devices (CCD cameras) and displays. The RGB model can be represented as a 3D-color space which describes emitted colors by using three *primary* colors [Maroto et al., 2006]:

- **R**ed of 700.0 nm (R);
- **G**reen of 546.1 nm (G);
- **B**lue of 435.8 nm (B).

The RGB model is called an *additive* model because all spectral colors from 380 nm to 780 nm can be formed by mixing of three primary colors in different proportions (Fig. 3.5).

Figure 3.5: Representation of additive color mixing

The RGB space can be illustrated as a cube with Cartesian coordinates (Fig. 3.6). This color representation allows us to calculate the maximum number of digital colors of the RGB color space. This model thus has the capability of representing 256^3= 16 777 216 colors.

According to the RGB model definition, color is described with three components: R, G and B. The value of these components is the sum of the respective sensitivity functions and the incoming light [Tkalcic & Jurij]:

$$R = \int_{\lambda} S(\lambda)R(\lambda)d\lambda \quad G = \int_{\lambda} S(\lambda)G(\lambda)d\lambda \quad B = \int_{\lambda} S(\lambda)B(\lambda)d\lambda \qquad (3.1)$$

where

$S(\lambda)$ is the light spectrum,

$R(\lambda)$, $G(\lambda)$ and $B(\lambda)$ are the sensitivity functions for the R, G and B sensors respectively.

Despite the fact that the RGB color model is simple, it has shortcoming in its practical application; since the RGB values depend on the sensitivity function of the capturing device the RGB model is device- and illuminant-dependent.

Other different color spaces can be obtained from the RGB space through linear or non-linear transformations. Review of the most widely used RGB color spaces and transformations can be found in [Pascal, 2003]. In this work, mainly the RGB space and HSV color spaces were applied.

The HSV color space (Fig. 3.6) is a transformation of the RGB color space and defines colors in terms of *hue*, *saturation* and *value*. The hue of a color is in actual fact its name (i.e. red, blue, pink or some combination such as greenish, etc). The saturation of a color is its purity property that represents its position on a scale from achromatic white to the pure hue. The value describes how light or dark the color is (it can also be called brightness) [Field, 2004]. The benefit of the HSV model is that hue and saturation components are similar to the way humans perceive colors. Thus some artists prefer to use this model.

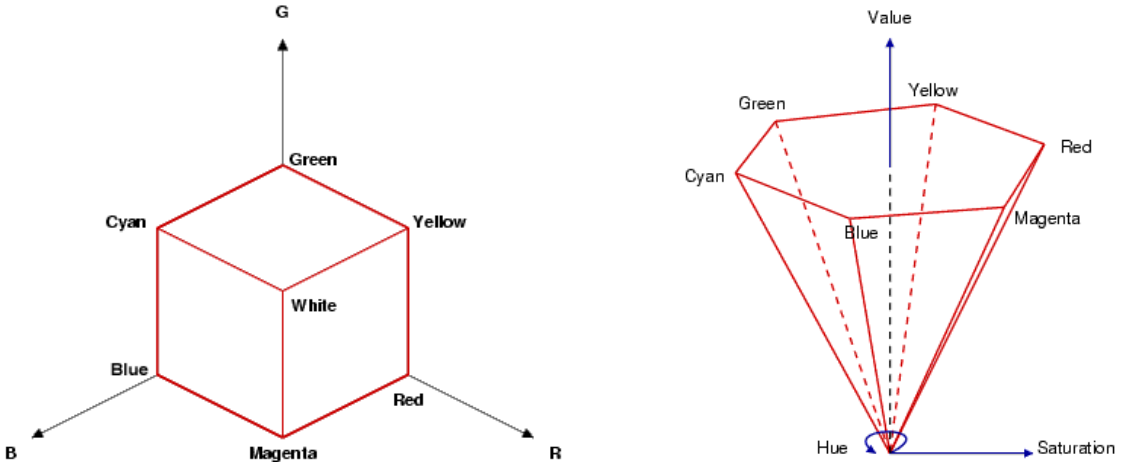

Figure 3.6: The RGB and HSV color models

A digital image is composed of pixels. To store the digital image, it is required to divide it into a grid of pixels. Each pixel represents the color at a single point in the image. It is defined by the amount of red, green and blue colors in the RGB space, for instance.

Hence the whole image results in an array of pixels sometimes called a *bitmap*. The density of pixels of a digital image is known as its *resolution*.

As pointed out before, color occurs as an event of three participants – a light source, an object and observer – but color also takes place only in human mind. We can measure the stimulus, i.e. light incoming to eyes and derive the response produced by the stimulus. For this purpose different types of measurement devices are used. All of them measure the light reflected or transmitted through a surface by using detectors. There are three main instruments namely densitometers, colorimeters, spectrophotometers. The differences between the three instruments are type and numbers of filters they use and their detectors sensitivity [Fraser et al., 2003].

Densitometers measure the degree to which surfaces absorb light (density). They are sufficient to measure darkness or lightness.

Colorimeters are devices used in colorimetry which measure colorimetric values in numbers that model the responses of the cone in the human eye. Colorimetry is the science that describes color in numeric models and predicts color match as human eyes perceive it. Modern colorimetry is based on the colorimetric system of the CIE. The CIE is a body of international color scientists. This organization provides a number of standard references and color spaces for defining colors [Fraser et al., 2003].

Spectrophotometry uses spectral imaging system to measure spectral reflectance which is the ratio between the intensity of light falling on an object and the reflected light [Fraser et al., 2003]. Nowadays the spectral reflectance provides the most accurate data regarding a color's characteristics.

3.3. Spectral imaging

The interest in spectral imaging has grown during the last few years. Nowadays, the applications of spectral imaging can be found in various fields of science and industry. The main benefit of spectral imaging is accuracy of the image acquisition. Imaging by spectral systems allows reproduction of the precise colors (exact spectral reflectance) and compensates for changes in illumination. Such a feature is useful for many applications

such as remote sensing, astronomy, food inspection, printing, study of illumination changes in natural scene, agrobiology and biochemistry.

Basically, the spectral imaging systems allow the acquisition of spectral images with high number of spectral channels. The main advantage of spectral imaging over digital imaging is that the reflected light from the object is captured in a great number of narrow spectral bands through the ultraviolet, visible and infrared part of the electromagnetic spectrum. Thus, the spectral image can be represented as a set of monochrome images referring to the different wavelength which leads to a greater amount of data, useful for detailed study of objects.

Of all the various spectral imaging systems, the line scanning based spectral camera ImSpector V10E (Fig. 3.7) was used for the measurement of spectral reflectance of fish skin samples in this study. This was to facilitate the analysis of the spectral reflectance of carotenoids-based colors.

Figure 3.7: ImSpector V10E spectral camera

Since the color of an object depends on its spectral reflectance $r(\lambda)$ and the spectral radiance of the illuminant can be represented as a function $l(\lambda)$, we can define the radiance of reflected light $f(\lambda)$ as the following equation [Hardeberg, 1999]:

$$f(\lambda) = r(\lambda) \cdot l(\lambda) \tag{3.2}$$

Schematically model is illustrated in Fig. 3.8.

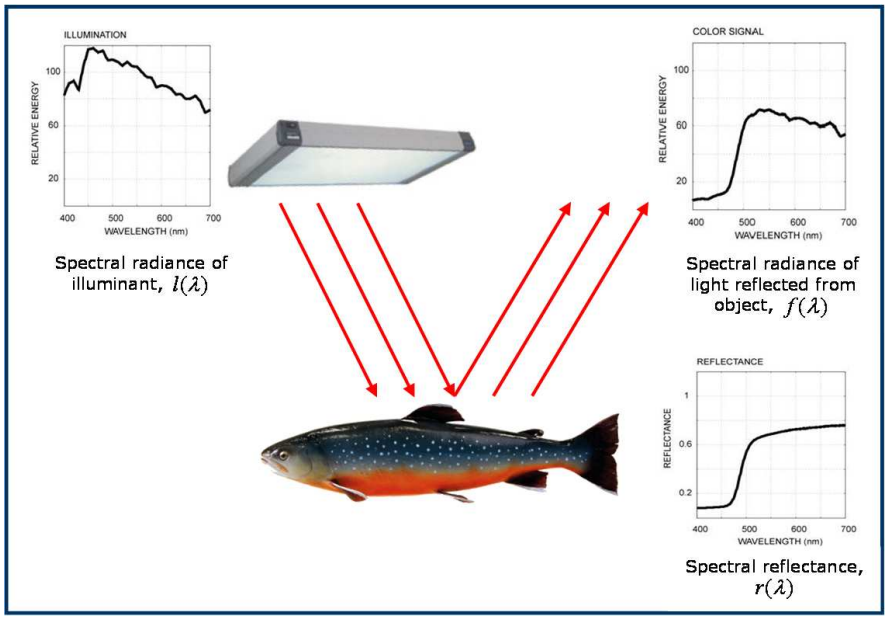

Figure 3.8: A simple spectral model for the interaction between light and the object

In spite of all the benefits of spectral imaging, there are also several disadvantages. A large volume of data, expensiveness of spectral devices and duration of image acquisition are significant limitations. In special applications and due to these limitations, a spectral reconstruction is needed which can be based on a variety of methods.

3.4. Spectra reconstruction

The color research of fish is such a case where the spectral image acquisition of living fish is highly problematic, especially for processing time and living animals' constraints (movements, limited time outside of water). Thus, as one of the solutions the spectra reconstruction from CCD camera responses is applied.

There are numbers of methods for enhancing reconstruction's performance such as kernel methods, Wiener estimation, Principal Component Analysis, radiance basis functions, neural networks, Self Organizing Map, numerical methods, look-up table methods. Review of the most popular estimation methods can be founded in literature [Heikkinen et al., 2007; Hardeberg, 1999; Baronti et al., 1998; Bochko et al., 2007].

In this work the polynomial transformation method for spectra reconstruction was applied. In different literature this method can be referred to as least squares polynomial

regression method [Heikkinen et al., 2007] or the method using multiple regression analysis [Bochko et al., 2007]. The polynomial model is a popular method used in color science for color calibration problems. In our case the color calibration of the digital camera can be determined by the following approximation problem [Jetsu et al., 2006]:

$$X \cdot W \approx Y \tag{3.3}$$

where X – matrix containing RGB values of the camera ($X \in \Re^{l \times 3}$);

Y – matrix containing spectra reflectance values ($Y \in \Re^{l \times n}$);

l - number of samples;

n - number of components in the spectrum;

W – transformation matrix mapping matrix X to matrix Y.

In this model, unknown coefficients can be calculated from least-squares approximation based on pseudo-inverse method [Jetsu et al., 2006]. In general, simple first order model are not be adequate to characterize the spectra data. First-order sets of linear equations can be extended to higher order polynomial by adding and combining cross-products and higher-order terms to matrix X, such as *RG*, *GB*, *RB*, R^2, G^2, B^2… to establish the best-fit transformation.

To perform this reconstruction procedure of polynomial transformation, a training set and test set are used. The training set is used to compute the transformation matrix W from RGB values to reflectance spectra. The training set is a set of matrix X and Y with known RGB values and reflectance spectra. Usually, for the training set the standard color checker charts are used such as Gretag Macbeth ColorChecker and Munsell Book which provide known reference colors.

With the matrix of spectral reflectance and a matrix with corresponding RGB values we can find matrix X by multiplying both sides of the equation by the inverse of the matrix X (i.e. X^{-1}). This is possible only for a square matrix. However, the approximation method can be used to compute the pseudo-inverse of a non-square matrix. In Matlab, the function *pinv* is applied [Westland & Ripamonti, 2004].

$$W = pinv(X) \cdot Y \tag{3.4}$$

The main limitations of the polynomial transformation model are illuminant and camera-dependency. Thus, for each combination of light source and type of digital camera, different transformation matrices needed to be computed.

3.5. Spectral reconstruction accuracy

In order to define the best order of the polynomial, some measurement of errors dependant on the particular solution needs to be defined. Ideally, the model should predict color with minimal errors. The process of spectral reconstruction (estimation) includes the statistical analysis of reconstructed spectra, estimation of error and minimization of error. To evaluate estimation accuracy, i.e. the difference between original (measured by spectral device) and estimated spectra from camera responses two types of spectral metrics were used in this work:

- CIELAB ΔE error for colorimetric color difference [Kohonen, 2002]

$$\Delta E = \sqrt{(L^* - \tilde{L}^*)^2 + (a^* - \tilde{a}^*)^2 + (b^* - \tilde{b}^*)^2} \tag{3.5}$$

where

L^*, a^*, b^* are CIELAB values calculated from original spectra;

$\tilde{L}^*, \tilde{a}^*, \tilde{b}^*$ are CIELAB values calculated from estimated spectra.

Table 3.1: Practical interpretation of CIELAB ΔE is represented by Hardeberg [Hardeberg, 1999]

ΔE	**Effect**
<3	Hardly perceptible
3<6	Perceptible, but acceptable
>6	Not acceptable

- Root Mean Squared Error (RMSE) for spectral color difference [Jetsu et al., 2006]

$$RMSE = \sqrt{\frac{\sum_{i=1}^{n} (s(i) - \tilde{s}(i))^2}{n}} \tag{3.6}$$

where

n is number of wavelength component in spectra

s is the original spectrum

$\tilde{s}$ is reconstructed spectra

The main purpose of this study is accuracy of spectral reconstruction rather than good colorimetric results. Thus, optimal model for spectral estimation should be chosen in respect of average value of RMSE error.

4. SPECTRAL RECONSTRUCTION TESTING AND SELECTION OF THE BEST MODEL FOR POLYNOMIAL REGRESSION

As mentioned before, the main goal of this study was to find a way to approximate the carotenoids amount of Arctic charr species based on fish skin spectra. In this work the correlation was examined and numerical expression of the correlation was established.

A way for acquisition of a spectral image of fish without taking long time with spectral camera is to reconstruct it from regular digital RGB images. For this purpose the *polynomial regression method* was suggested (see section 3.4). The crucial points in this method are defining the training set (what and size of set) and choosing the order of the approximation function for obtaining a smooth solution. The choice of polynomial function should base on statistical analysis of results and minimization of errors. The spectral reconstruction process of fish has been carried out in several stages (Fig. 4.1). In this chapter the different polynomial regression models were tested with various sets for training and testing purpose.

4.1. Spectral reconstruction of Macbeth chart

For testing the polynomial transformation model, I first used the standard Macbeth ColorChecker with 24 patches as a training and test set. According to the algorithm (see Fig. 4.1) the matrices X and Y have to be determined to find the transformation matrix W. Spectral reflectance values of the Macbeth chart were taken for matrix Y. spectral measurements of the Macbeth chart have been done with Perkin-Elmer lambda 9 UV/VIS/NIR spectrometer in 380 - 780 nm range wavelengths (Fig. 4.2). Thus, matrix Y of size 24x81 with 5 nm step in visible range was obtained.

For matrix X, RGB values should be taken. A set of digital images of Arctic charr with Macbeth ColorChecker (Fig. 4.3) was used to obtain RGB values of Macbeth chart from corresponding patches. For this, the mean values of the RGB for each patch were calculated by using the digital images and matrix X of size 24 x 3 was obtained.

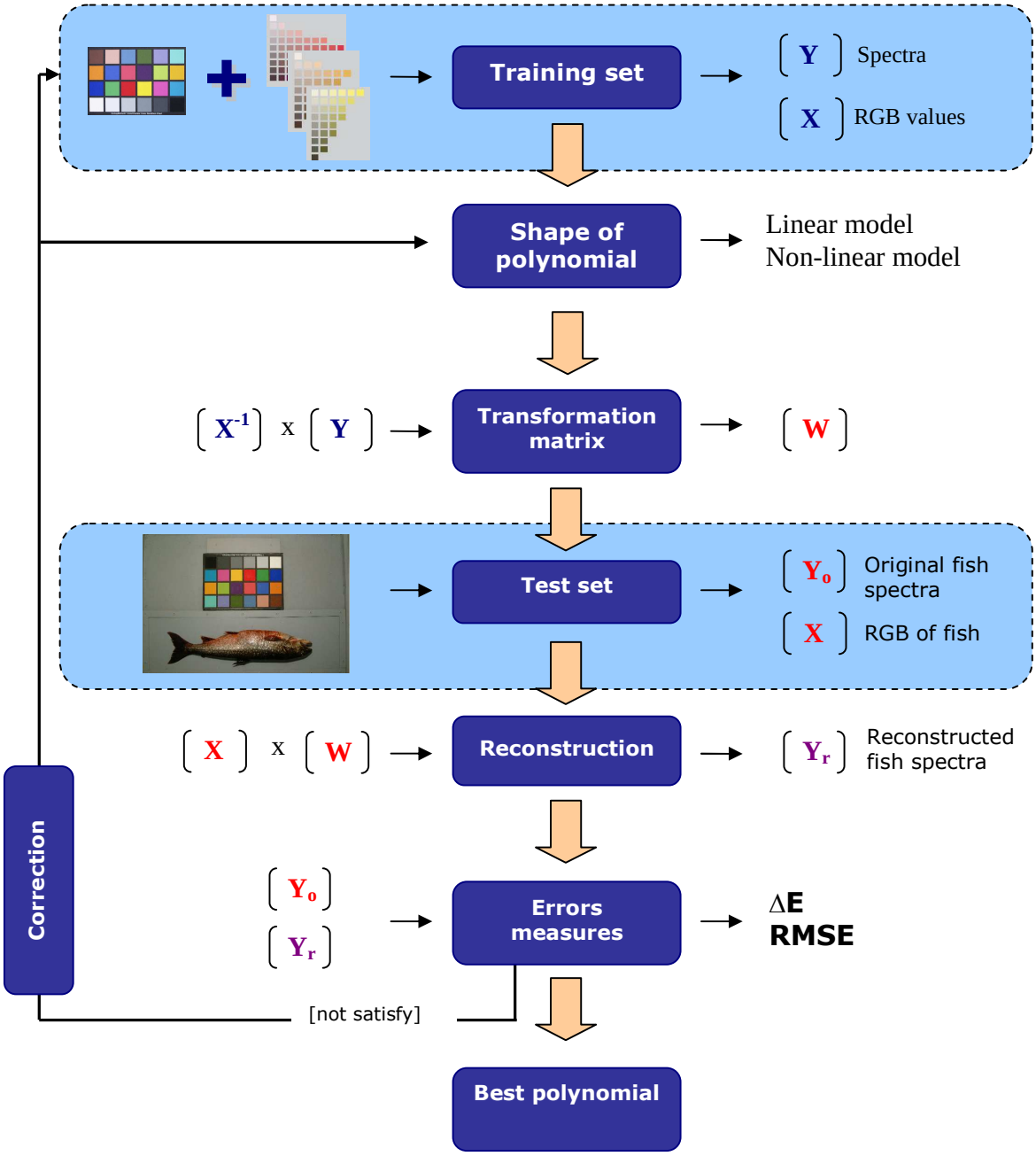

Figure 4.1: Algorithm for the least squares polynomial regression method for reconstructing fish spectra

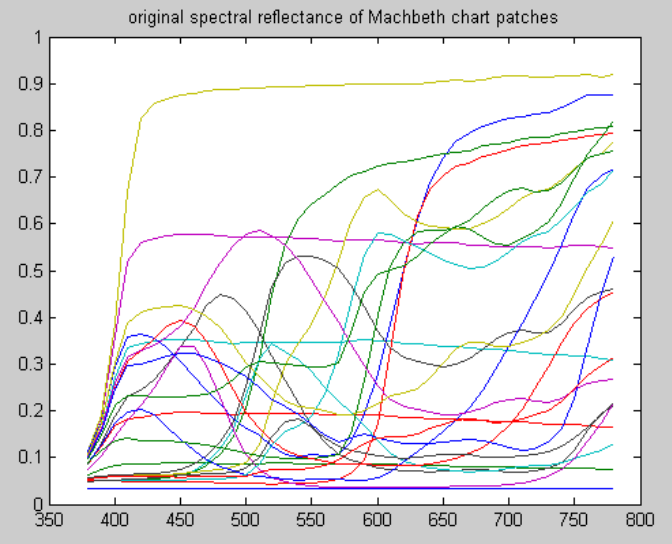

Figure 4.2: Spectral reflectance of the Macbeth chart

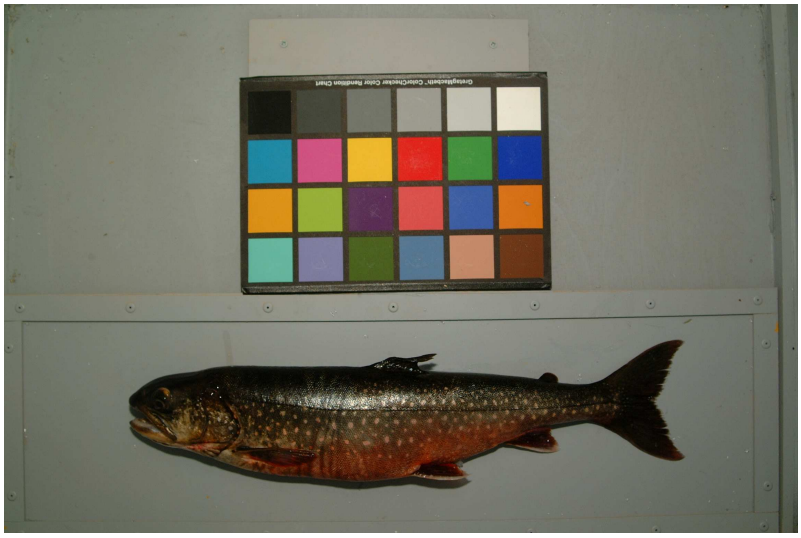

Figure 4.3: RGB image of Arctic charr with Macbeth ColorChecker

The shapes of different polynomials can be varied and tested for their accuracy performance. A chain of polynomials containing three to twenty terms for transformation matrix calculations was determined.

For calculating the transformation matrix W, first, second and third order degree polynomials are used with 3, 10 and 20 terms, respectively. Moreover, second and third order polynomials include a constant term, 1 (Table 4.1).

Table 4.1: Three types of polynomials used for fish spectra reconstruction

# terms	Polynomial
	1st order
3	R G B
	2nd order
10	R G B R^2 G^2 B^2 RG RB GB 1
	3rd order
20	R G B R^2 G^2 B^2 RG RB GB 1 RGB RGG RBB GRR GBB BRR BGG R^3 G^3 B^3

Thus, matrix dimensions for solving the approximation problems for the Macbeth chart (24 patches, 81 channels) are illustrated in Table 4.2.

Table 4.2: Matrix dimension for different polynomials

Order of polynomial	Spectra	RGB values	Matrix transformation
	<l x n>	<l x k>	<k x n>
	Y =	**X** *	**W**
1st	<24x81>	<24x3>	<3x81>
2nd	<24x81>	<24x10>	<10x81>
3rd	<24x81>	<24x20>	<20x81>
	where **l** – number of samples, **n** – number of wavelength components in spectra, **k** – number of terms in polynomial.		

The equations used for calculating matrix W with the Macbeth chart (24 samples) as training set shown below:

Linear model (3 terms):

$$[Y] = [R \quad G \quad B] \cdot [W]$$

$$\begin{bmatrix} y_{1,1} & \cdots & y_{1,81} \\ \vdots & \ddots & \\ y_{24,1} & \cdots & y_{24,81} \end{bmatrix} = \begin{bmatrix} x_{1,1} & x_{1,2} & x_{1,3} \\ \vdots & \ddots & \\ x_{24,1} & x_{24,2} & x_{24,3} \end{bmatrix} \cdot \begin{bmatrix} w_{1,1} & \cdots & w_{1,81} \\ w_{2,1} & \ddots & \\ w_{3,1} & \cdots & w_{3,81} \end{bmatrix}$$

2nd order polynomial (10 terms):

$$[Y] = [R \quad G \quad B \quad R^2 \quad G^2 \quad B^2 \quad RG \quad GB \quad RB \quad 1] \cdot [W]$$

$$\begin{bmatrix} y_{1,1} & \cdots & y_{1,81} \\ \vdots & \ddots & \\ y_{24,1} & \cdots & y_{24,81} \end{bmatrix} = \begin{bmatrix} x_{1,1} & \cdots & x_{1,10} \\ \vdots & \ddots & \\ x_{24,1} & \cdots & x_{24,10} \end{bmatrix} \cdot \begin{bmatrix} w_{1,1} & \cdots & w_{1,81} \\ \vdots & \ddots & \\ w_{10,1} & \cdots & w_{10,81} \end{bmatrix}$$

The 3rd order polynomial equation is formed in the same manner; by adding cross-product (RGB, RGG, RBB, GRR, GBB, BRR, BGG) and higher-order terms (R^3, G^3, B^3).

Computing these in Matlab resulted in the transformation matrices W for each polynomial case. Then, the estimated spectra were obtained by applying matrixes W to RGB values of the Macbeth chart by using the pseudo-inverse method. Fig. 4.4 illustrates the results obtained with 20 terms (3rd polynomial order).

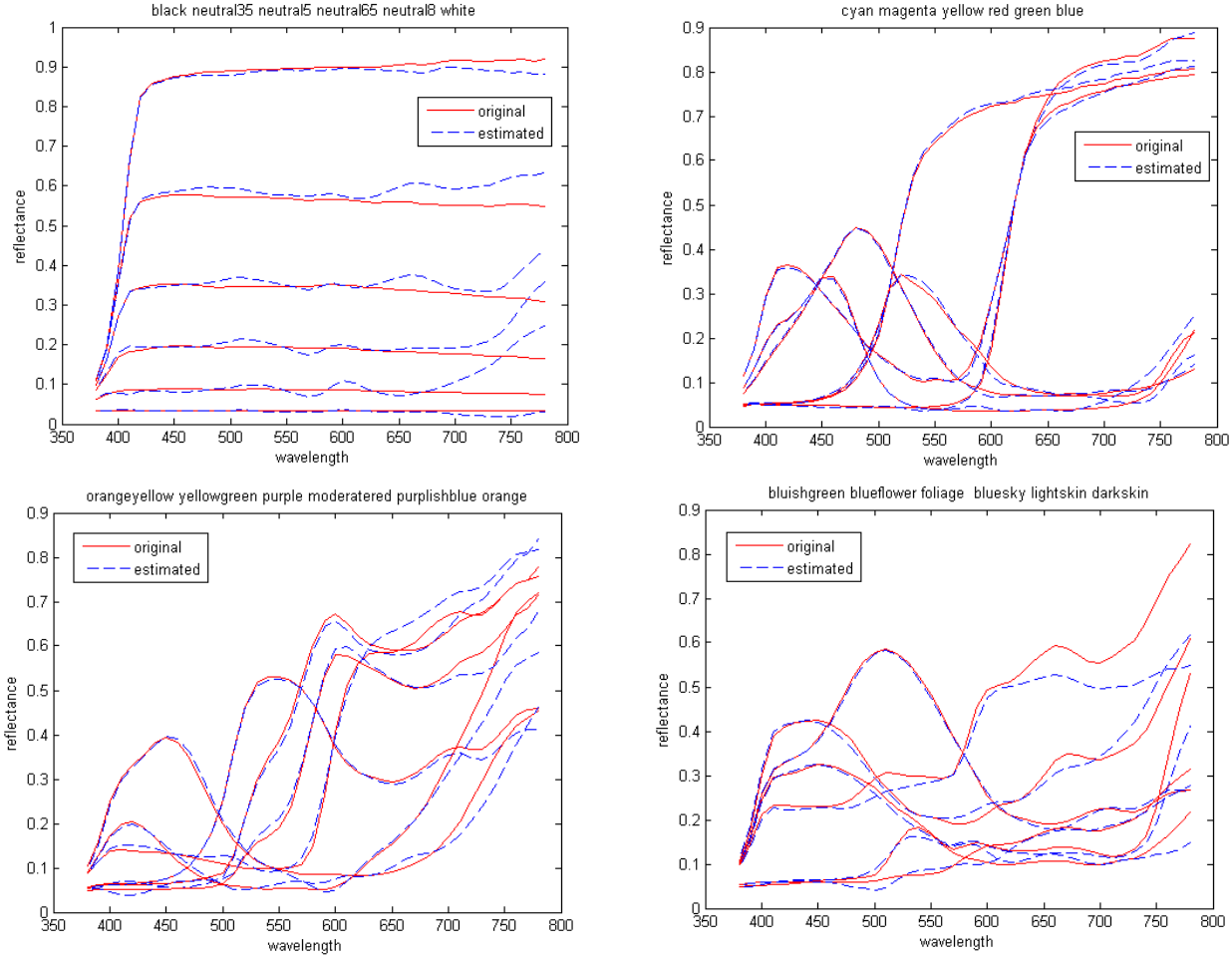

Figure 4.4: The Macbeth chart – spectral estimation with 20 terms: solid line: original spectra, dashed line: estimated spectra

Evaluation the spectral accuracy was done with the calculation of ΔE and RMSE errors (3.5, 3.6). The results of the 2nd and 3rd order polynomials are shown in Fig. 4.5.

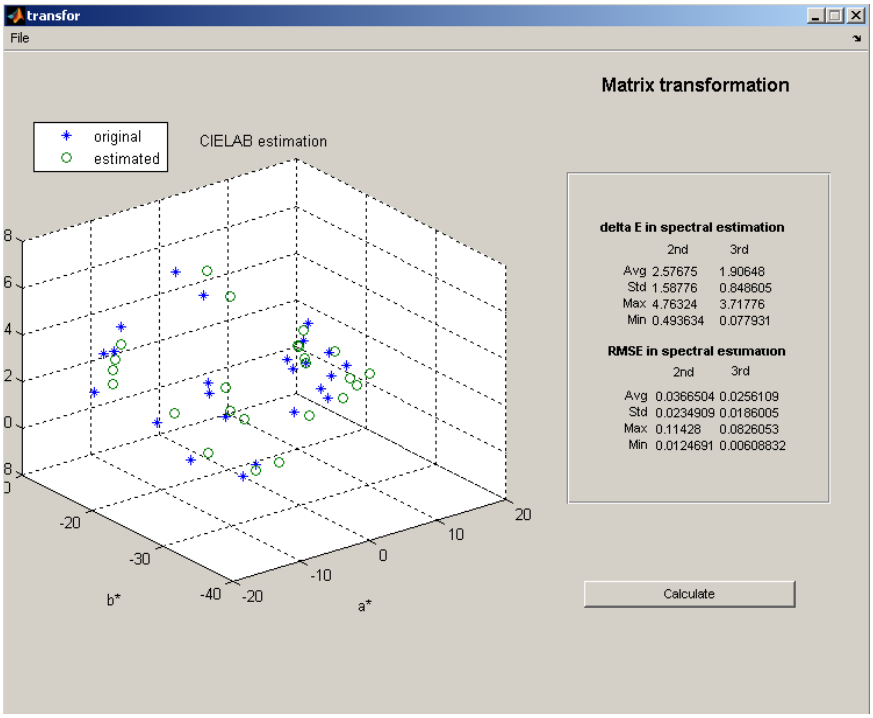

Figure 4.5: Spectral reconstruction accuracy calculation for Macbeth chart: Δ E, RMSE for 2nd and 3rd order polynomials and CIELAB estimation

Based on the analysis of error measures, it can be concluded that the least values of both types of errors have been obtained in the case of *the third order polynomial.* The mean of CIELAB ΔE error is equal to 1.9 which according to Hardeberg's interpretation (Table 3.1) is "hardly perceptible" (less than 3). The mean of RMSE is equal to 0.025 which is less than value in 2nd order.

This illustrates the result of polynomial regression spectra reconstruction from RGB values with the Macbeth chart as a training and test set. In this case we got an optimal result.

4.2. Fish spectra reconstruction with the Macbeth chart as a training set

Next, the polynomial transformation method was tested for reconstruction of the *fish spectra*. To test the method accuracy the Macbeth chart (24 samples) was used as a training set and the spectral image of fish as a test set. The testing was done in the following manner: the spectra of the Macbeth chart and fish were converted to sRGB with 'D65' light source and CIE 1931 system parameters. The obtained RGB values produced matrices X. then, 2^{nd} and 3^{rd} order polynomials were formed (as in section 4.1). In training stage the transformation matrix W was computed based on training set. Calculated matrix W was applied to sRGB image of the fish and sRGB image of the Macbeth chart with 10 and 20 terms of polynomials.

Fig. 4.6 demonstrates three images of the same fish. The upper one is the original spectral image converted into sRGB color space; below, on the left and on the right are reconstructed spectral images with 2^{nd} and 3^{rd} order polynomial and transformed into sRGB color space, respectively.

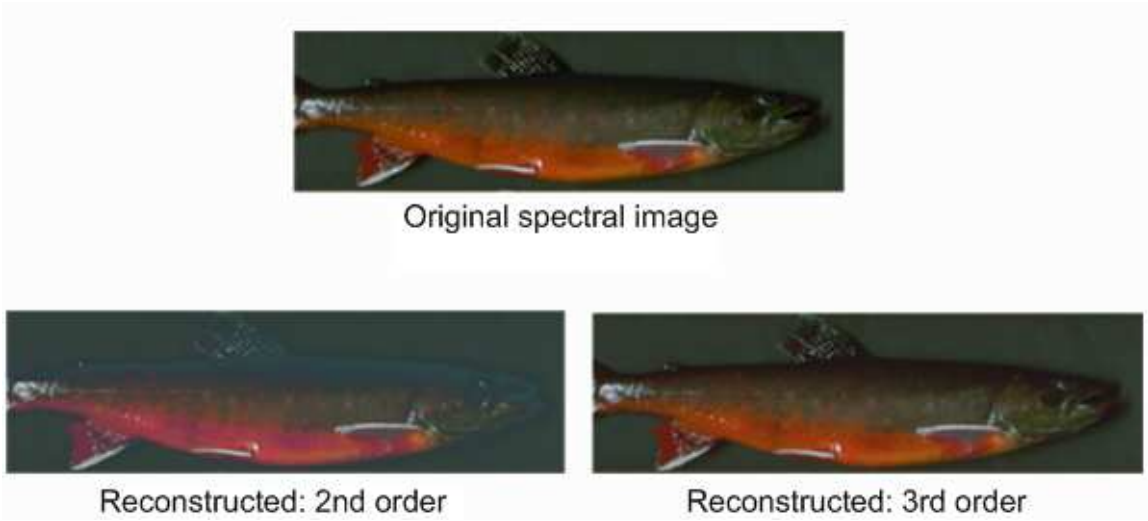

Figure 4.6: Original and reconstructed spectral images of fish

Next step in testing model is model evaluation. Two types of errors CIELAB Δ E and RMSE errors were calculated to check the accuracy of spectral reconstruction. As mentioned in section 3.5, the selection appropriate results were obtained in respect of the values of RMSE since we interested in accurate spectra estimation. The errors between

the original and reconstructed images in case of fish image and the Macbeth chart image are displayed in Table 4.3 and Table 4.4.

Table 4.3: The ΔE error in spectra reconstruction of the fish image and Macbeth chart

ΔE				
	Avg.	**Std.**	**Max.**	**Min.**
	Image of fish			
2nd order (10 terms)	9.1862	6.9114	31.1366	0.1041
3rd order (20 terms)	2.8097	2.8057	27.2516	0.003
	Training set			
2nd order (10 terms)	0.7511	0.5437	1.9430	0.1354
3rd order (20 terms)	0.0551	0.0576	0.2244	0.0021

Table 4.4: The RMSE error in spectra reconstruction of the fish image and Macbeth chart

RMSE				
	Avg.	**Std.**	**Max.**	**Min.**
	Training set			
2nd order (10 terms)	0.0354	0.0250	0.1229	0.0094
3rd order (20 terms)	0.0262	0.0225	0.0916	0.0026
	Image of fish			
2nd order (10 terms)	1.6078	2.2106	11.3326	0.1819
3rd order (20 terms)	3.186	3.5024	16.2798	0.2319

In summary: the color difference CIELAB ΔE in *the 3rd order polynomial* is less than the 2nd order polynomial and value 2.8097 is "hardly perceptible"; RMSE error in the *2nd order* is equal to 1.6078 which is less than in the 3rd.

This shows that the 3rd order polynomial with lower value of CIELAB color difference is better in case of the quality of color reproduction. This is shown in Fig. 4.6. As we are interested in accuracy of spectra reconstruction, the polynomial with lower value of RMSE should be used as a criterion for choice the appropriate polynomial model. Based on this the 2nd order polynomial gave the most accurate result.

Fig. 4.7 and 4.8 demonstrate the difference before and after spectra estimation of the Macbeth chart and the fish image, respectively. It is important to note that the original spectra reflectance of fish shown by blue line (Fig. 4.8) has a peak in the range between 350-400nm which can be explained by measurement error.

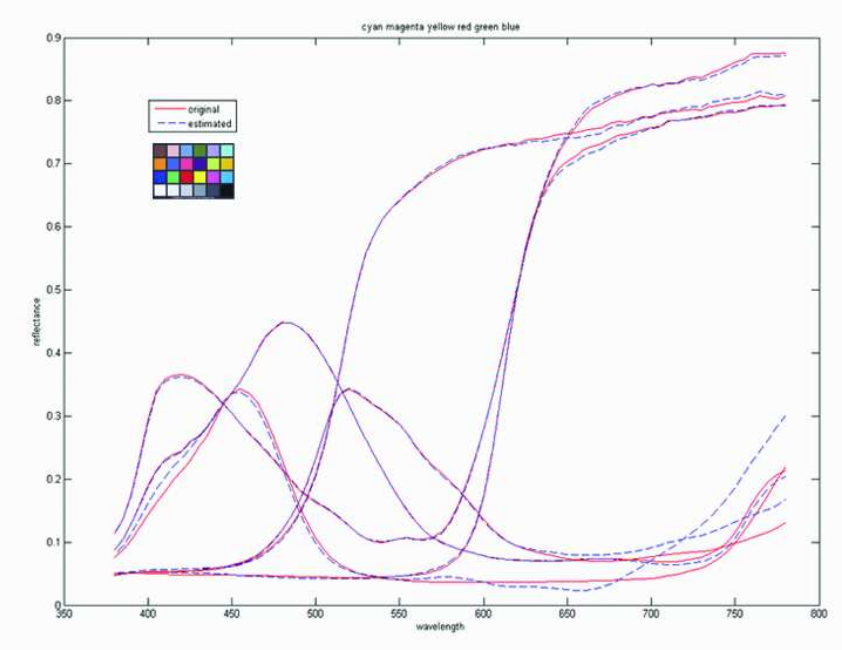

Figure 4.7: Macbeth chart: original spectra (solid line) and reconstructed spectra (dash line)

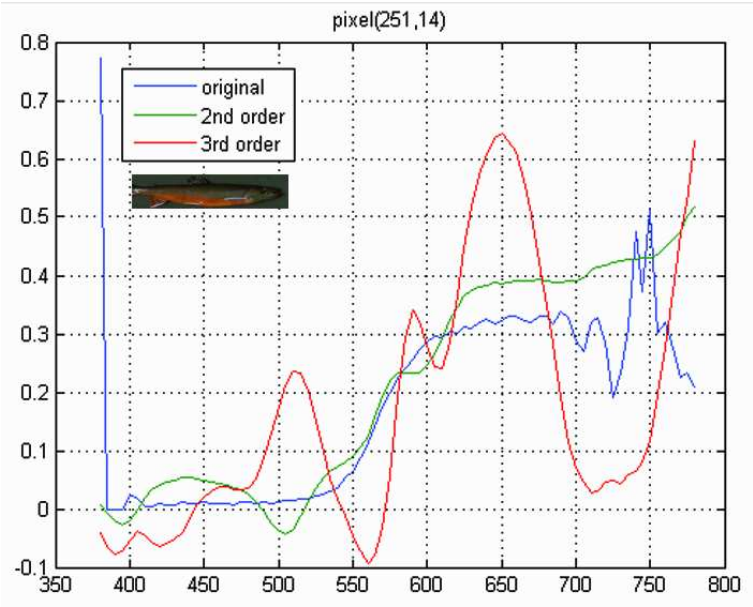

Figure 4.8: Fish image: original spectra (blue line), reconstructed with 2nd order (green line) and reconstructed with 3rd order (red line)

4.3. Fish spectra reconstruction with the Macbeth chart and part of the Munsell book as a training set

The next step to improve results and decrease spectral color difference within the spectral reconstruction was to increase the size of the training set. The samples from the Munsell book were chosen to be included to the training set. For this purpose yellow and red specimens were chosen as carotenoids-based colors. Finally, the training set was extended from 24 to 428 samples by consecutively adding yellow (YY), yellow-red (YR) and red (RR) patches from the Munsell book. Matrices X and Y in the training set and test set were built similarly as before, i.e. the spectral image were transformed to sRGB ('D65', CIE 1931). Reconstruction was done in a similar way with 10 and 20 term polynomials. RGB images of reconstructed fish image for the 2^{nd} and 3^{rd} order polynomials are illustrated in Fig. 4.9, compared against the RGB image calculated from the original spectra.

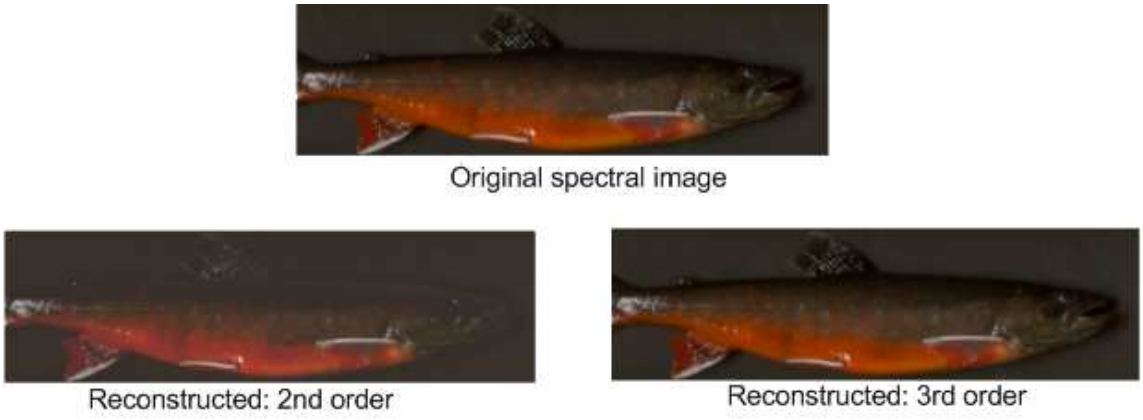

Figure 4.9: Original and reconstructed spectral images of fish using extended training set

Colorimetric and spectral color difference errors were calculated to evaluate result and compare with previous results (Tables 4.5 and 4.6).

Table 4.5: Colorimetric color difference after reconstruction

ΔE					
		Avg.	**Std.**	**Max.**	**Min.**
		Image of fish			
2^{nd} order (10 terms)	Macb	9.1862	6.9114	31.1366	0.1041
	Mac+XYY	7.7407	6.0777	28.2561	0.1058

ΔE					
		Avg.	**Std.**	**Max.**	**Min.**
	Mac+XYY+XYR	8.3574	6.4532	28.2481	0.0260
	Mac+YYRR(404)	8.2703	7.1867	31.8375	0.0360
3rd order (20 terms)	Macb	2.8097	2.8057	27.2516	0.003
	Mac+XYY	3.0271	3.5854	26.9802	0.0147
	Mac+XYY+XYR	3.2334	3.1669	27.0605	0.0054
	Mac+YYRR(404)	1.8174	2.9300	27.1408	0.0030
		Training set			
2nd order (10 terms)	Macb	0.7511	0.5437	1.9430	0.1354
	Mac+XYY	1.3823	1.8873	17.8670	0.0617
	Mac+XYY+XYR	1.0955	1.6314	18.0721	0.0821
	Mac+YYRR(404)	0.4700	0.5994	8.3434	0.0139
3rd order (20 terms)	Macb	0.0551	0.0576	0.2244	0.0021
	Mac+XYY	0.6849	1.3344	13.2440	0.0233
	Mac+XYY+XYR	0.5458	1.0999	13.9019	0.0116
	Mac+YYRR(404)	0.0571	0.1188	2.2247	0.0016

Table 4.6: Spectral color difference after reconstruction

RMSE					
		Avg.	**Std.**	**Max.**	**Min.**
		Training set			
2nd order (10 terms)	Macb	0.0354	0.0250	0.1229	0.0094
	Mac+XYY	0.0254	0.0168	0.1408	0.0032
	Mac+XYY+XYR	0.0276	0.0193	0.1554	0.0049
	Mac+YYRR(404 patch)	0.0188	0.0156	0.1620	0.0030
3rd order (20 terms)	Macb	0.0262	0.0225	0.0916	0.0026
	Mac+XYY	0.0222	0.0159	0.1007	0.0023
	Mac+XYY+XYR	0.0240	0.0184	0.1456	0.0020
	Mac+YYRR(404 patch)	0.0138	0.0139	0.1637	0.0016
		Image of fish			
2nd order (10 terms)	Macb	1.6078	2.2106	11.3326	0.1819
	Mac+XYY	1.5047	2.2076	11.0383	0.2475
	Mac+XYY+XYR	1.4981	2.1945	11.0646	0.2938
	Mac+YYRR(404 patch)	**1.4041**	1.9767	9.8274	0.1737
3rd order (20 terms)	Macb	3.186	3.5024	16.2798	0.2319
	Mac+XYY	1.5418	2.3626	10.9252	0.1089
	Mac+XYY+XYR	1.4258	2.3840	10.9380	0.1255
	Mac+YYRR(404 patch)	1.5349	2.1575	9.8115	0.0940

Fig. 4.10 and Fig. 4.11 show the original spectral reflectance curves of the fish image and reconstructed spectra for 2nd and 3rd order polynomials for chosen pixel.

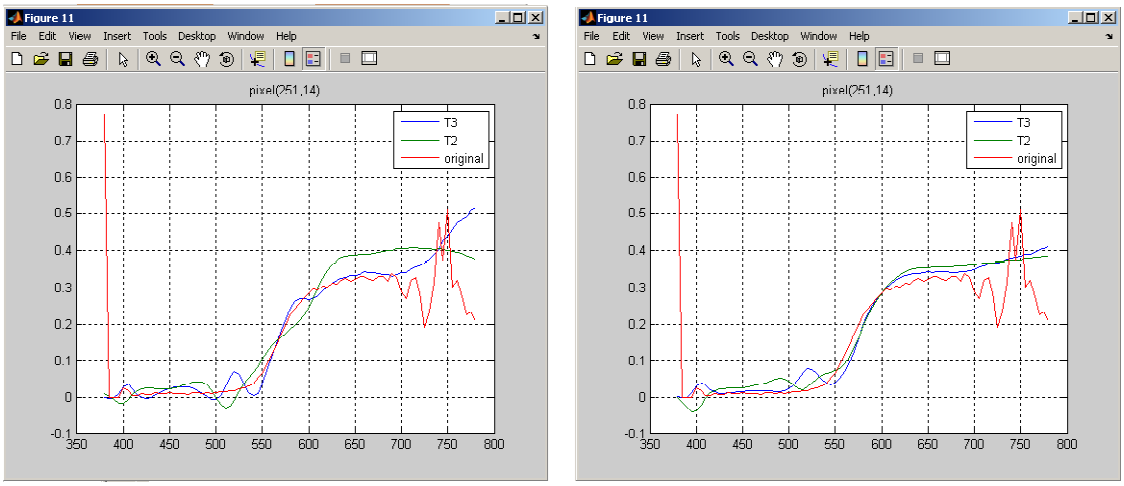

Figure 4.10: Original (red line) and reconstructed spectra of fish with 10 (green line) and 20 (blue line) terms, respectively. On the left, the training set is the Macbeth + YY; on the right is the Macbeth chart +YY+YR patches

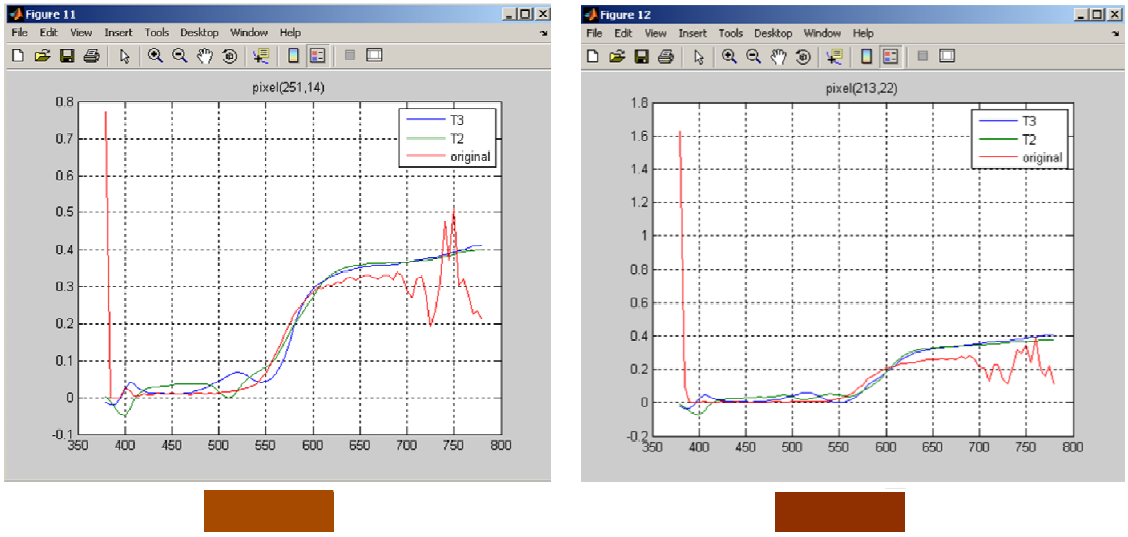

Figure 4.11: Original (red line) and reconstructed spectra of fish with 10 (green line) and 20 (blue line) terms, respectively, for different pixels. The training set is the Macbeth + YY + YR + RR. Below the graphs are colors of the pixels

Analysis of the fish spectra reconstruction revealed the following: CIELAB ΔE error decreased from 2.8097 to 1.8174 in the 3rd order which is still less than in the 2nd order polynomial; RMSE has the least value of error in *the 2nd order polynomial*, which

decreased from 1.6078 to 1.4041. With regard to the decreasing of RMSE values, spectral curves of the reconstructed spectra look smooth and closer to original.

Also, polynomial regression method was tested with a set of spectral images of fish skin samples measured by the spectral line camera ImSpector 10E. A description of all conducted measurements is considered in Chapter 5. Testing of the reconstruction method was performed with the training set consisting the Macbeth chart and part of the Munsell book for the 2nd and 3rd order polynomials.

Tables 4.7 – 4.12 show the colorimetric (ΔE) and spectral color difference (RMSE) errors between the original and estimated spectra of different fish skin samples.

Table 4.7: Spectral estimation accuracy for skin sample # 11

ΔE					
		Avg.	**Std.**	**Max.**	**Min.**
2nd order (10 terms)	Macb	10.6588	5.3871	22.804	1.0054
	Mac+YYRR	7.2169	4.4481	18.762	0.2563
3rd order (20 terms)	Macb	2.255	1.877	10.833	0.0826
	Mac+YYRR	1.2367	0.9662	7.8765	0.3212
RMSE					
2nd order (10 terms)	Macb	0.5179	0.3244	2.0126	0.1044
	Mac+YYRR	**0.3159**	0.1464	0.7605	0.0947
3rd order (20 terms)	Macb	1.9526	1.5631	7.8154	0.1032
	Mac+YYRR	0.3341	0.171	0.7227	0.0621

Table 4.8: Spectral estimation accuracy for skin sample # 14

ΔE					
		Avg.	**Std.**	**Max.**	**Min.**
2nd order (10 terms)	Macb	9.1913	4.6515	20.6443	0.7431
	Mac+YYRR	6.0646	3.6474	16.4245	0.3555
3rd order (20 terms)	Macb	1.6734	1.2929	9.792	0.1663
	Mac+YYRR	0.9056	0.4854	6.0003	0.2114
RMSE					
2nd order (10 terms)	Macb	0.5208	0.3355	1.9847	0.0854
	Mac+YYRR	**0.2989**	0.1353	0.7741	0.092
3rd order (20 terms)	Macb	1.7189	1.293	5.9625	0.0944
	Mac+YYRR	0.3254	0.1781	0.7619	0.0612

Table 4.9: Spectral estimation accuracy for skin sample # 10

ΔE					
		Avg.	**Std.**	**Max.**	**Min.**
2nd order (10 terms)	Macb	2.2833	2.2596	14.0901	0.0905
	Mac+YYRR	1.4028	1.2312	9.9955	0.42
3rd order (20 terms)	Macb	0.3441	0.3428	4.1933	0.0023
	Mac+YYRR	0.445	0.2606	2.7709	0.0184
RMSE					
2nd order (10 terms)	Macb	0.3835	0.3063	1.6232	0.0738
	Mac+YYRR	**0.2246**	0.1044	0.5408	0.0629
3rd order (20 terms)	Macb	0.7983	0.6225	2.1389	0.0518
	Mac+YYRR	0.296	0.1587	0.6033	0.0528

Table 4.10: Spectral estimation accuracy for skin sample # 2

ΔE					
		Avg.	**Std.**	**Max.**	**Min.**
2nd order (10 terms)	Macb	0.5867	0.3341	1.7043	0.0928
	Mac+YYRR	0.2449	0.1011	0.9747	0.0149
3rd order (20 terms)	Macb	0.2009	0.0978	0.3766	0.0014
	Mac+YYRR	0.1534	0.0692	0.3573	0.0067
RMSE					
2nd order (10 terms)	Macb	**0.3135**	0.1812	0.7583	0.0636
	Mac+YYRR	0.469	0.3878	1.1527	0.0584
3rd order (20 terms)	Macb	0.4224	0.5151	2.8739	0.063
	Mac+YYRR	0.4886	0.417	1.2334	0.0584

Table 4.11: Spectral estimation accuracy for skin sample # 23

ΔE					
		Avg.	**Std.**	**Max.**	**Min.**
2nd order (10 terms)	Macb	2.3862	1.6275	15.7696	0.3347
	Mac+YYRR	1.1018	1.0402	11.3691	0.2654
3rd order (20 terms)	Macb	0.3407	0.2272	4.2915	0.0619
	Mac+YYRR	0.5297	0.1093	1.5705	0.1132
RMSE					
2nd order (10 terms)	Macb	0.5329	0.4997	2.5974	0.1046
	Mac+YYRR	**0.2506**	0.1142	0.4594	0.0834
3rd order (20 terms)	Macb	0.7191	0.4987	2.2754	0.0733
	Mac+YYRR	0.3262	0.1892	0.7001	0.0678

Table 4.12: Spectral estimation accuracy for skin sample # 22

ΔE					
		Avg.	**Std.**	**Max.**	**Min.**
2nd order (10 terms)	Macb	1.2567	0.9872	9.6891	0.0798
	Mac+YYRR	0.9561	0.4298	6.0255	0.2339
3rd order (20 terms)	Macb	0.1872	0.1214	1.5369	0.0011
	Mac+YYRR	0.3448	0.1451	1.8923	0.0154
RMSE					
2nd order (10 terms)	Macb	0.3836	0.34	1.7442	0.0723
	Mac+YYRR	**0.2355**	0.1191	0.6111	0.0586
3rd order (20 terms)	Macb	0.6686	0.4745	1.5025	0.0578
	Mac+YYRR	0.3452	0.2059	0.7032	0.0558

Fig. 4.12 compares results of spectra estimations performed with different training sets: in the first case, the training set is the Macbeth chart with 24 samples (on the left) and in second case is extended training set (the Macbeth chart and the Red-Yellow part of the Munsell book). It can be concluded that the reconstructed spectra with extended training set (on the right) looks closer to the original than the one on the left. The reconstructed spectrum of the 2nd order polynomial is smoother than with 3rd order polynomial.

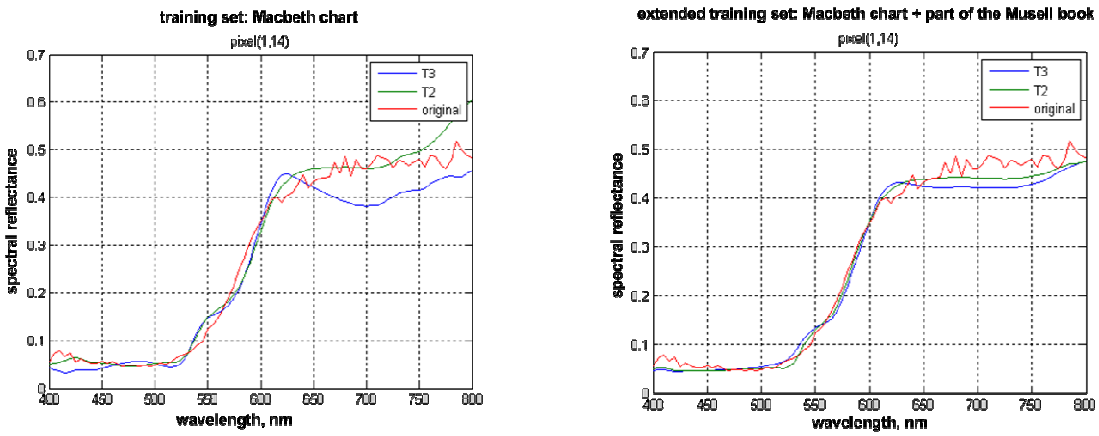

Figure 4.12: Comparison between the original (red line) and estimated fish spectra of the 2nd (green line) and the 3rd order polynomial (blue line) with different training sets

4.2. Summary

In this chapter we considered polynomial regression spectra reconstruction from RGB values. This method was tested with the 2nd and 3rd order polynomials with 10 and 20 terms, respectively. In the training phase, the Macbeth chart color checker (24 samples) and Red-Yellow specimens of Munsell book (404 samples) were used to improve the reconstruction. As a testing set, sRGB values of the Macbeth chart and sRGB images of fish and measured skin samples of Arctic charr were utilized.

Analysis of the results for different training sets demonstrated that by increasing the size of the training set *the spectral reconstruction accuracy was improved.* The testing process showed that the 2nd order polynomial model with extended training set produces the most accurate reconstruction of the tested method. Thus, this model was chosen as the most accurate model for spectra estimation of the Arctic charr from RGB values. The digital images of fish and of the training set must be acquired under the same condition, however. Calculation of corresponding transformation matrix W must be conducted for only certain conditions, i.e. the light source and type of camera. To estimate spectra from RGB images of fish taken under various conditions, corresponding transformation matrices must be computed.

5. EXAMINATION OF CORRELATION BETWEEN CAROTENOIDS AMOUNT IN FISH SKIN AND THEIR SPECTRA

5.1. Measurements and pre-processing of spectral images

As described in Chapter 2, the carotenoids of Arctic charr are important pigments which are responsible for specific fish coloration. One of the aims this study is to examine the correlation mechanism between carotenoids amount in fish skin and their reflectance spectra.

For this purpose the spectral measurements of the Arctic charr's skin were made in order to obtain spectral information of the skin coloration which varied in hue. Spectral images of fish skin were acquired by the spectral camera, ImSpector V10E with D65 illumination in the visible range of wavelengths 400 – 800 nm with a 5 nm step. The specimens of fish skin selected were of various colors to encompass as much hue of fish skin coloration as possible (Fig. 5.1). The size of each sample was approximately 10x10 mm (a size required in pigment analysis). All the measurements were conducted with skin samples of frozen and fresh fish. Fig. 5.2 shows the spectral image of a fish skin sample converted to sRGB and a spectra curve of a chosen pixel.

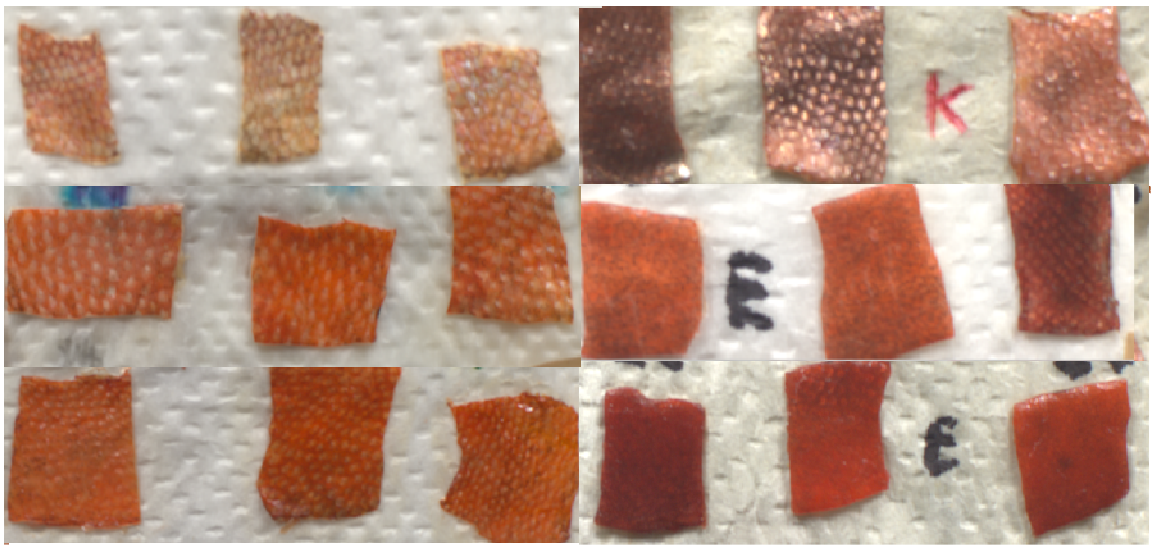

Figure 5.1: A color variety of measured fish skin

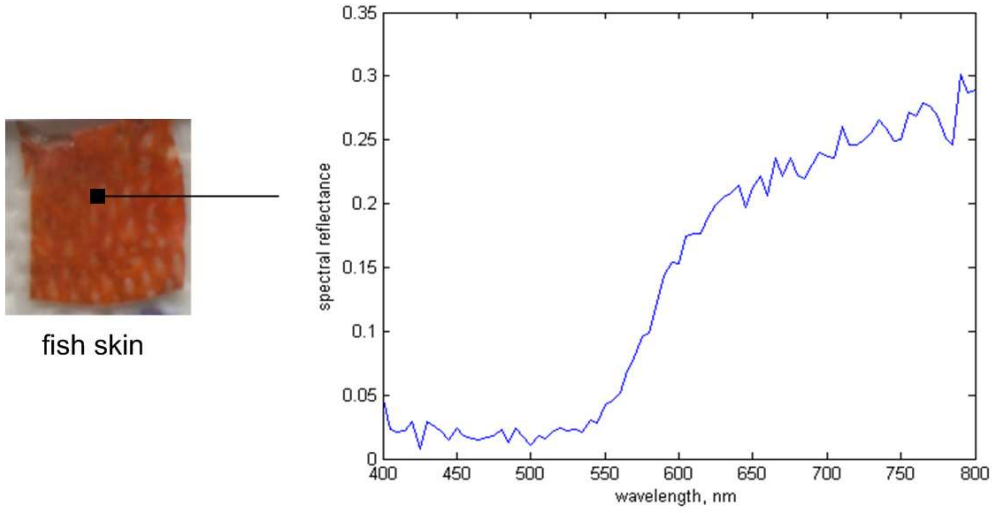

Figure 5.2: Skin sample of fish and spectral reflectance of chosen pixel

Moreover, to conduct spectral reconstruction with a chosen in Chapter 4 the polynomial model with training set, RGB images of skin samples were taken by a digital camera (Canon) under D65 illumination. Since selected training set contains Macbeth chart (24 patches) and Munsell book pages (YY, YR and RR), RGB images of them were acquired under the same with fish skin conditions.

All the spectral images of skin samples were subjected to further processing. Average values of spectral reflectance were calculated for each fish skin sample to match them to carotenoids amount of corresponding skin sample and to examine their correlation. As a result, matrix of spectral reflectance was computed where the number of rows corresponds to the number of samples. Example of the fish skin samples and their corresponding average spectral reflectance is shown in Fig. 5.3 and Fig. 5.4. All the measured skin samples of fish and the computed means spectral reflectance for each one are shown in Appendix 1.

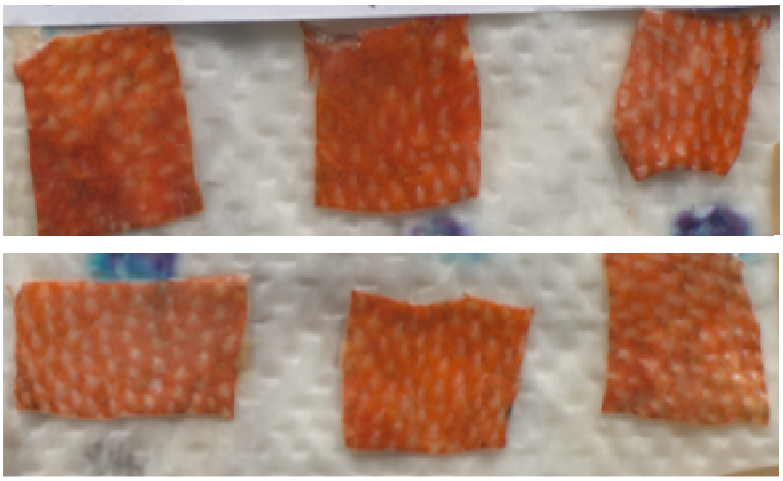

Figure 5.3: Spectral images of skin samples (numbers: 13-18) of frozen fish converted to sRGB

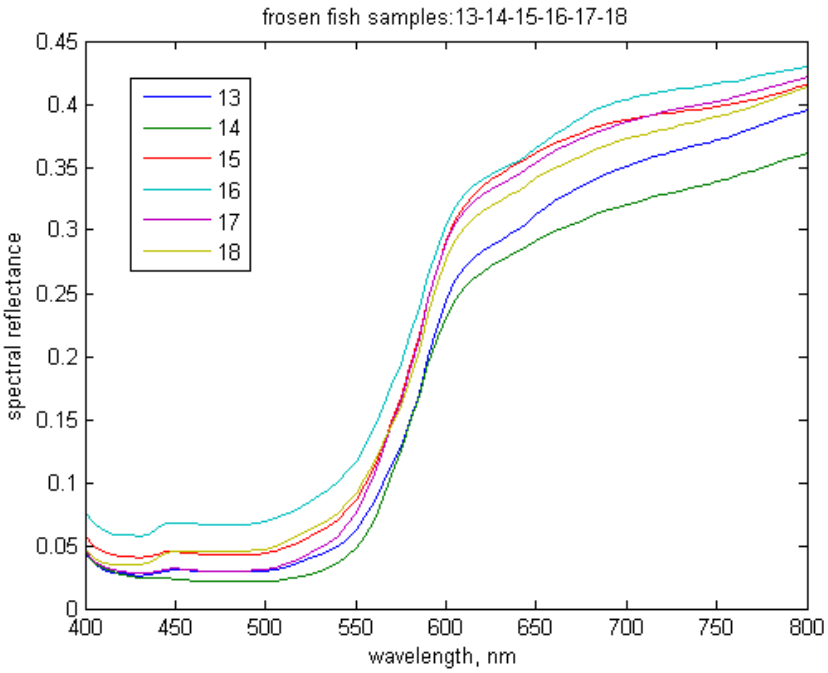

Figure 5.4: Average spectral reflectance for skin samples (numbers: 13-18)

The analysis of the mean reflectance demonstrated that the skin samples with brighter red coloration have lower values of spectral reflectance rather than samples with dull coloration (Fig. 5.5).

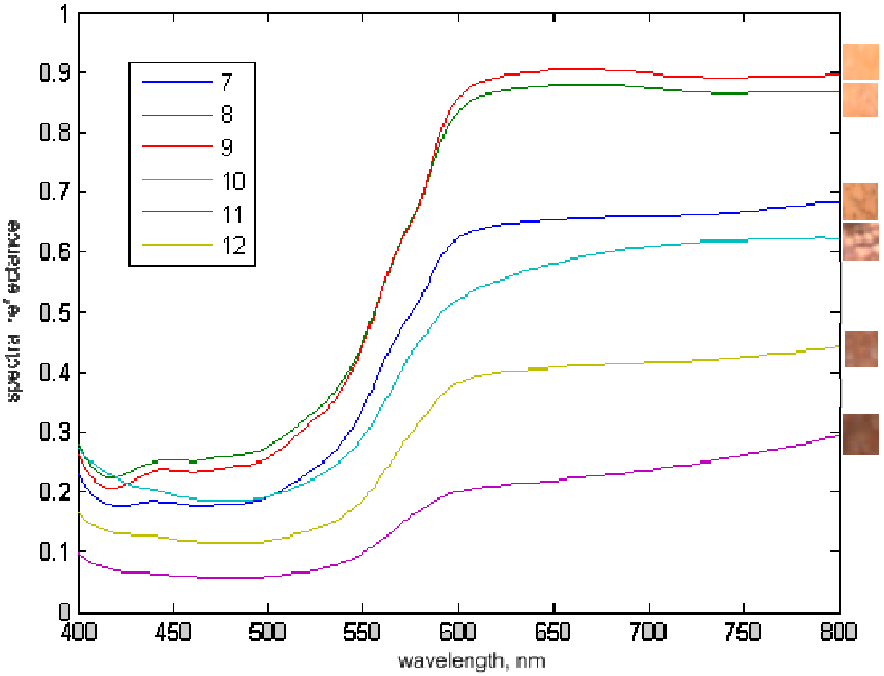

Figure 5.5: Spectral reflectance and corresponding color of fish skin (on the right); saturation of skin color is increasing from up to down

After the measurement session and digital imaging, the fish samples were exposed to chemical analysis for extraction of the carotenoids. The pigment analysis was conducted by the Department of Biology of University of Joensuu. Carotenoid pigment was extracted by an established method described by Scalia *et al* [Scalia et al., 1989]. The process was performed in several steps. The samples were placed into test-tubes and each fish skin sample was weighted (Fig. 5.6). Carotenoids, to be more precise – astraxanthin, were dissolved from fish skin with acetone and were filtered under reduced pressure (Fig. 5.7). A special formula was used to calculate the concentration of the extracted astraxanthin. As a result a data set with the amounts of astraxanthin for each skin sample was obtained.

Figure 5.6: Measuring the weight of skin samples

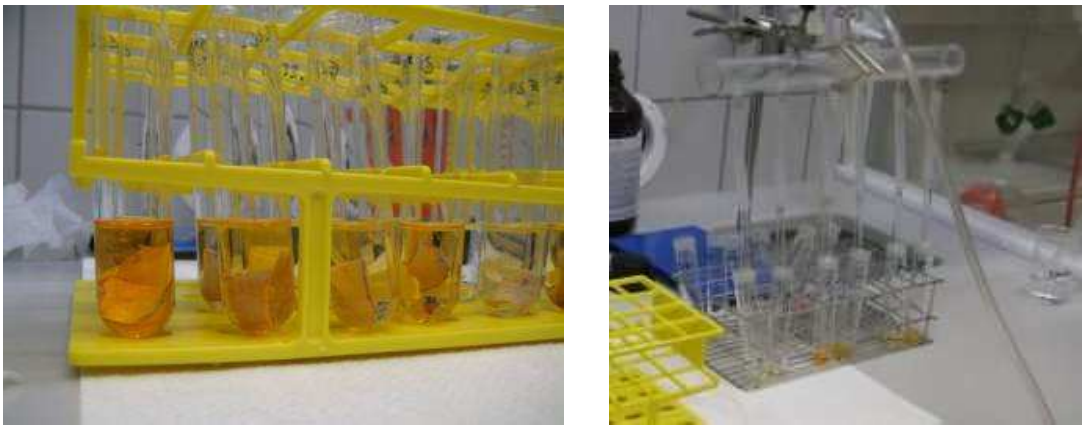

Figure 5.7: Dissolving carotenoids with acetone (on the left) and filtering the pure carotenoids under reduced pressure (on the right)

5.2. Correlation in frozen and fresh sets of fish skin samples

As input we had two data sets to analyze – data with the average spectral reflectance and data with measured carotenoids concentration of each skin sample. To examine the relationship between them, ratio analysis of reflectance spectrum [Chappelle et al., 1992] was used to estimate bands sensitive to the pigment. Blackburn [Blackburn, 1998] suggested that the optimal individual waveband for carotenoids estimation is located at 470 nm. Thus, a carotenoids-specific index R800/R470 was derived for this purpose,

where R800 and R470 are the reflectance (R) at the corresponding wavelengths, respectively, as a quantitative measure of carotenoids.

As mentioned before two types of fish were used (frozen and fresh fish) for measurements and pigment analysis. The sample size of frozen fish was 30. It must be noted that the sample size was altered for the fresh fish sample because of the presence of noise. The sample size of fresh fish set was as such reduced from 42 to 32. The noise can be explained by the errors introduced by spectral measurement and pigment analysis. In addition, a glossiness of fresh fish skin caused the spectral reflectance to increase to values greater than 1 which created problems in the spectral measurements and digital imaging process.

Thus, the relationships between the reflectance spectra and carotenoids amount, were verified separately with frozen and fresh fish data sets and are plotted in Fig. 5.8 and Fig. 5.9.

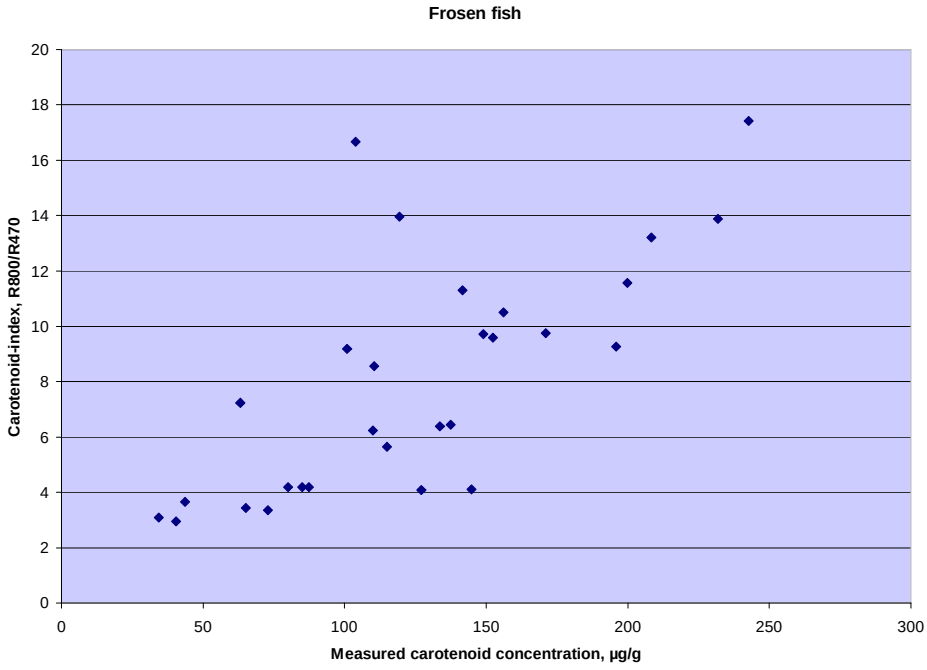

Figure 5.8: Carotenoids-index reflectance R800/R470 is compared to measured carotenoid concentration in frozen fish

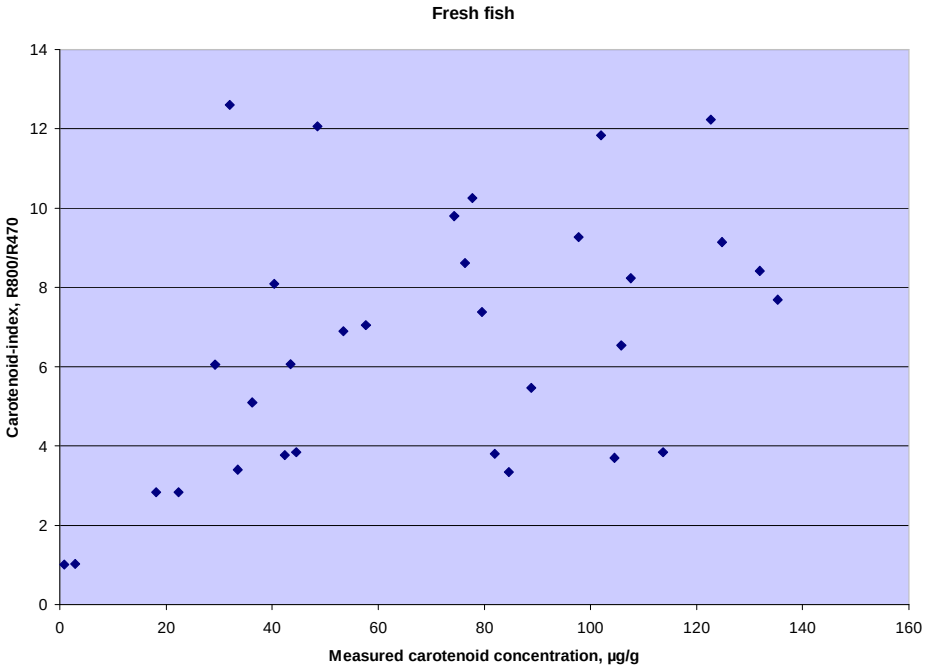

Figure 5.9: Carotenoids-index reflectance R800/R470 is compared to measured carotenoid concentration in fresh fish

To evaluate the strength of the correlation between the reflectance ratio and amount of carotenoids quantitatively, the correlation coefficients[1] and coefficient of determination[2] were calculated for frozen and fresh fish sets (Table 5.1). Positive values of correlation coefficients indicate a positive direction of correlation; which means that when one variable (i.e. amount of carotenoids) tends to increase, the other variable (Carotenoids-index, R800/R470) also tends to increase. Values of the correlation coefficient show the significant correlation between two variables. A correlation coefficient of 0.7280 for a sample size of 30 frozen fish gave a 95% confidence interval of ranging from 0.50 to 0.86. Similarly, for fresh fish a correlation coefficient of 0.5925 was obtained for a sample size of 32, with a 95% confidence interval ranging from 0.31 to 0.79. The values of the coefficients signify that for frozen fish, 53% of the variance in the carotenoids-

[1] Correlation coefficient (r) measures the strength and direction of the relationship between two or more variables [Statsoft Electronic Textbook].
[2] Coefficient of determination (r^2) gives the proportion of the variance of one variable that is predictable from the other variable [Statistic 2, Correlation] .

index R800/R470 is "explained" by the amount of carotenoids in fish skin; for the fresh fish it is 31.1%.

Table 5.1: Correlation and determination coefficients for sets of frozen and fresh fish

Fish	Correlation coefficient, r	Coefficient of determination, r^2
Frozen	0.7280	0.5300
Fresh	0.5925	0.3510

After analyzing the sets separately, the two sets of frozen and fresh fish were combined (Fig. 5.10). The relationship between the carotenoids-ratio and measured carotenoids concentration was plotted and a linear regression equation was found (Fig. 5.11). The calculated correlation coefficient equaled 0.679 showing a significant correlation between the two variables in combined set of frozen and fresh fish. The 95% Confidence Interval on the population with a sample size of 62 ranged from 0.52 to 0.80. The calculated determination coefficient equaled 46.12%, implying that 46.12% of the variability in the carotenoids-ratio can be explained by the variability in carotenoids concentration.

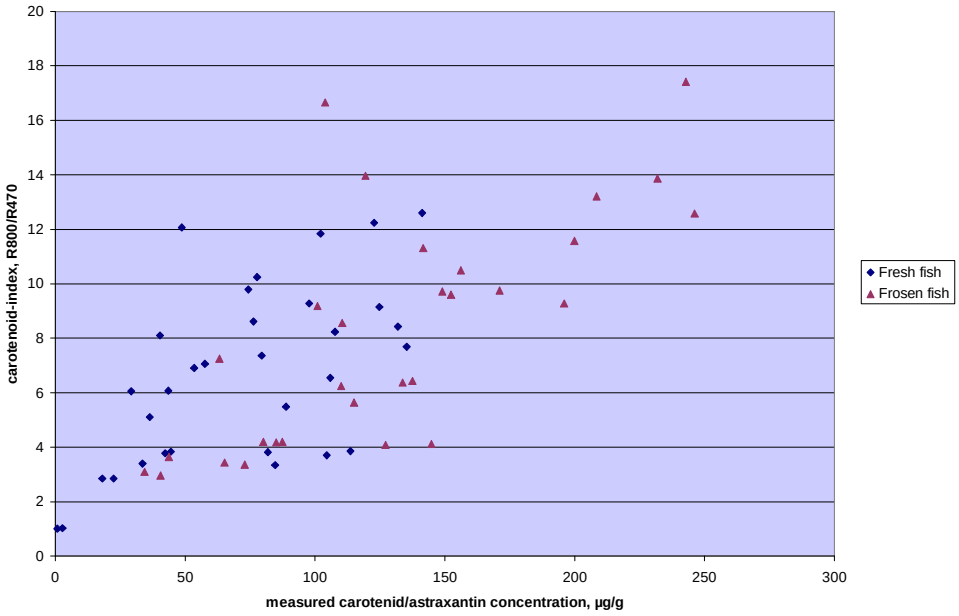

Figure 5.10: Carotenoids-index reflectance R800/R470 is compared to measured carotenoid concentration for combined set of frozen and fresh fish

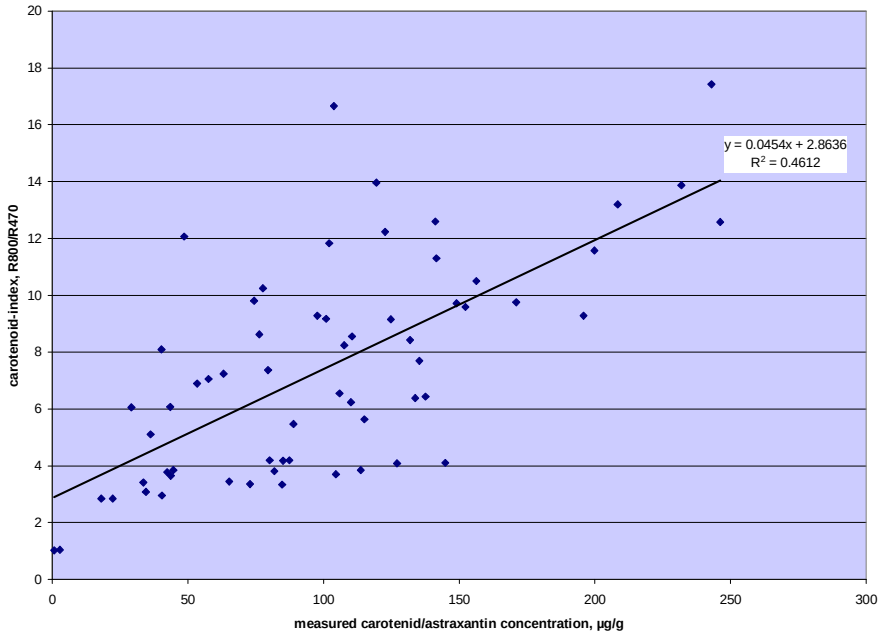

Figure 5.11: Linear regression found between carotenoids-index and measured carotenoids concentration for combined set of frozen and fresh fish

5.3. Summary

In this chapter the correlation between amount of carotenoids in fish skin and their spectral reflectance was examined. As a metric of spectral reflectance for carotenoids, reflectance indices R800/R470 sensitive to the carotenoids were chosen. Frozen and fresh fish sets were investigated separately and together. Analyses of the results showed a positive correlation between the amount of carotenoids in fish skin and their spectral reflectance. Calculated correlation coefficients indicated a significant correlation ($r>0.5$). In addition, the correlation in the frozen fish set was higher than in fresh fish. It should be noted that the measurements and pigment analysis of fresh fish turned out to be more complicated than frozen fish. Glossiness of the fresh fish skin, errors of the measurements and analysis led to the elimination of some samples.

A combined set of frozen and fresh fish with sample size of 62 was studied by regression analysis. A linear regression line was plotted with the following equation: $y=0.0454x+2.8636$. Using this, the amount of carotenoids can be predicted from the

spectral ratio of spectral reflectance of fish skin without an expensive or long pigment analysis process. Thus, a nondestructive technique for the assessment of carotenoids content from spectral reflectance in the Arctic charr was developed.

5. DISCUSSION AND CONCLUSION

In this work we tried to apply known color imaging technique for particular issue from real life. The main aim of this work was to facilitate work of biology scientists in the investigation of the Arctic charr species. The key point in studying is assessment of carotenoids amount which conveys valuable information about fish vitality and health conditions in evolutionary biological research, particularly. To avoid an expensive and long chemical analysis required a sacrificing of fish specimens, an affordable methods to approximate amount of carotenoids in fish skin by using spectral information was proposed. The method involves a reconstruction spectral reflectance from RGB images and allows conducting a *non-destructive* process for approximation amount of carotenoids based on spectral carotenoids-ratio.

During this research a polynomial regression method was investigated to improve accuracy of the reconstruction of fish spectra. A polynomial model and extended training set enhanced spectral reconstruction were determined. Relationships between carotenoids amount and spectral reflectance were investigated in frozen and fresh skin sets, separately. The significant positive correlation between carotenoids concentration and spectral reflectance of samples being measured was found. The examination showed higher correlation in set of frozen. We faced with challenges with fresh fish processing. A glossiness of fresh fish skin was an obstacle in correct measurements. A preparation of the samples of fresh fish (to cut and separate a thin layer of skin from a body) according to required parameters for pigment analysis was problematically. A weight of skin sample (with a required size) exceeded the maximum allowable weight. All these led to errors and noise in evaluation. Unlike the fresh fish, spectral measurements and pigment analysis of the frozen fish samples was performed without any difficulties. Taking into account this aspect and higher correlation coefficient, it can be assumed that frozen fish is preferable for utilizing for carotenoids investigation. But, from another hand, a process of freezing and defreezing can affect to carotenoids pigment content. Since this area is now well-studied, it is difficult to make a conclusion about frozen fish.

The conducted examination of correlation between carotenoids amount in fish skin and their spectra confirmed a *feasibility* of the proposed method for quantify of carotenoids

by using spectral information. But the future developments of this method are needed. To see if there are any significant changes in the RMSE errors, testing of other spectral reconstruction methods are required. A re-examination of the relationship between carotenoid amount in fish skin and their spectra with larger number of samples would improve the results of correlation. Moreover, studying of the fresh fish and investigation new way to enhance the spectral measurements and pigment analysis process would recommend for improving results. Probably, any changes in the spectral reconstruction method and type of regression in prediction of carotenoid amount based on spectral information may produce better results in the future.

REFERENCE

Aario S, Silvén O. and Kauppinen H. *Vitality and reflectance spectra of living plants: experiments.* Proc. 3rd International Conference on Multispectral Color Science (MCS'01), June 18-21, pp. 31-34, Joensuu, Finland, 2001.

Arctic Centre-Information Service. Internet WWW-page, URL (03.02.2008): http://arcticcentre.ulapland.fi/docs/Arctic_fish_species.pdf

Baronti, S., Casini, A., Lotti, F. and Porcinai, S. *Multispectral imaging system for the mapping of pigments in works of art by use of principal-component analysis*. Applied optics, 37(8), pp. 1299-1309, 1998.

Blackburn, G.A. *Quantifying chlorophylls and carotenoids from leaf to canopy scales: An evaluation of some hyper-spectral approaches.* Remote Sensing of Environment, 66(3), pp. 273-285. 1998.

Bochko V., Tsumura N. and Miyake Y. *A Spectral color imaging system for estimating spectral reflectance of paint.* Journal of Imaging Science and Technology, 51(1), pp.70-78, 2007.

Chappelle, E. W., Kim, M. S. and McMurtrey, J. E. *Ratio Analysis of Reflectance Spectra (RARS): an algorithm for the remote estimation of the concentrations of chlorophyll A, chlorophyll B, and carotenoids in soybean leaves*. Remote Sensing Environ., 39, pp.239-247, 1992.

Chatzifotis, S., Pavlidis, M., Jimeno, C.D., Vardanis, G., Sterioti, A., Divanach, P. *The effect of different carotenoid sources on skin coloration of cultured red porgy (Pagrus pagrus).* Aquaculture Research 36 (15), pp.1517–1525, 2005.

Field, G. G. *Color and Its Reproduction. Fundamentals for the Digital Imaging and Printing Industry.* 3rd edition. 2004.

Fraser, B., Murphy, C., Bunting F. *Real World Color Management: Industrial-Strength Production Techniques.* 2003.

Gitelson, A. A, Zur, Y., Chivkunova, O. and Merzlyak, M.N. *Assessing carotenoid content in plant leaves with reflectance spectroscopy.* Photochemetry and Photobiology. 75(3),

pp.272-281, 2002.

Grether, G.F., Kasahara, S., Kolluru G.R. and Cooper E.L. *Sex-specific effects of carotenoid intake on the immunological response to allografts in guppies (Poecilia reticulata).* Proceedings of the Royal Society of London B, 271, pp.45-49, 2004.

Hardeberg, J.Y. *Acquisition and reproduction of colour images: colorimetric and multispectral approaches*. Ph.D dissertation (Ecole Nationale Supérieure des Télécommunications), Paris, France, 1999.

Heikkinen, V., Jetsu, T., Parkkinen, J., Hauta-Kasari, M., Jaaskelainen, T. and Lee S.D. *Regularized learning framework in the estimation of reflectance spectra from camera responses*. Journal of the Optical Society of America A, 24(9), pp. 2673-2683, 2007.

Hofmann, C.M., Cronin, T.W. and Omland, K.E. *Melanin coloration in New World orioles II: ancestral state reconstruction reveals lability in the use of carotenoids and phaeomelanins*, Journal of Avian Biology, 38(2), pp.172, March 2007.

Hofmann, C.M., Cronin, T.W. and Omland, K.E. *Using spectral data to reconstruct evolutionary changes in coloration: carotenoid color evolution in New World orioles*. Evolution, 60, pp.680-1691, 2006.

Humphries, J. M., Graham, R. D. and Mares, D.J. *Application of reflectance colour measurement to the estimation of carotene and lutein content in wheat and triticale.* Journal of Cereal Science, 40, pp.151-159, 2004.

Jetsu, T., Heikkinen, V., Parkkinen, J., Hauta-Kasari, M., Martinkauppi, B., Lee, S.D., Ok, H.W. and Kim, C.Y. *Color Calibration of Digital Camera Using Polynomial Transformation*. In Proceedings of CGIV2006 - 3rd European Conference on Colour in Graphics, Imaging, and Vision, Leeds, UK, pp. 163-166, June 19-22, 2006.

Karttaikkuna Oy, karttoja kaikille. Internet WWW-page, URL (03.02.2008): http://www.karttaikkuna.fi/susa/3.pdf

Kohonen, O. *Spectral imaging systems*. M.Sc. thesis. March 2002.

Lozano, G. A. 1994. *Carotenoids, parasites, and sexual selection*. Oikos 70: 309-311.

Maroto, J.A., Valverde, C.M., Peñalver and Tejero, J.E. Bueno-González. *Description of additive colour mixing exhibits by using PC-designed Maxwell discs.* Physics Education, 41(5), pp. 448-452(5), September 2006.

Martinkauppi, B., Doronina, E., Piironen, J., Jaaskeläinen, T. and Parkkinen, J. *Novel system for semiautomatic image segmentation of arctic charr.* Journal of electronic imaging, 16(3), pp.033012-8, Joensuu, Finland, 2007.

Måsvaer, M., Liljedal, S., Folstad, I., *Are secondary sex traits, parasites and immunity related to variation in primary sex traits in the Arctic charr?* Processing of the Royal Society B, 271(suppl 3), pp. 40–42, 2004.

McGraw, K. J., Hudon, J., Hill, G. E., and Parker, R. S. *A simple and inexpensive chemical test for behavioral ecologists to determine the presence of carotenoid pigments in animal tissues.* Behavioral Ecology and Sociobiology 57, pp.391-397, 2005.

Pascal, D. *A review of RGB color spaces…from xyY to R'G'B'*. The BabelColor company, Canada, 2002-2003.

Saks, L., McGraw, K., Hõrak, P. *How feather colour reflects its carotenoid content.* Functional Ecology, 17, pp.555–561, 2003.

Scalia, S., Isaksen, M. and Francis, G.W. *Carotenoids of the arctic charr, Salvelinus alpinus* L. Journal of Fish Biology, 34, pp.969–970, 1989.

Statistic 2, Correlation. Internet WWW-page, URL (03.02.2008): http://mathbits.com/mathbits/TISection/Statistics2/correlation.htm

Statsoft Electronic Textbook, Internet WWW-page, URL (03.02.2008): http://www.statsoft.com/textbook/stathome.html

Sugimoto, M. and Oshima, N. *Introduction: Biology of pigment cells in fish.* Microscopy Research and Technique, 58(6), pp.433-434, 2002.

Tkalčič, M. and Tasič J.F. Color spaces – perceptual, historical and applicational background", EUROCON 2003. Computer as a Tool, The IEEE Region 8(1), pp. 304-308, Sept. 2003.

von Schantz, T., S. Bensch, M. Grahn, D. Hasselquist & H. Wittzell. *Good genes, oxidative stress and condition-dependent sexual signals* Processing of the Royal Society B, 266, pp.1-12, 1999.

Westland, S., Ripamonti, C. *Computational Colour Science using MATLAB.* John Wiley & Sons, Ltd, 2004, 220 pages.

APPENDIX 1: Spectral measurements results

FROSEN FISH SAMPLES

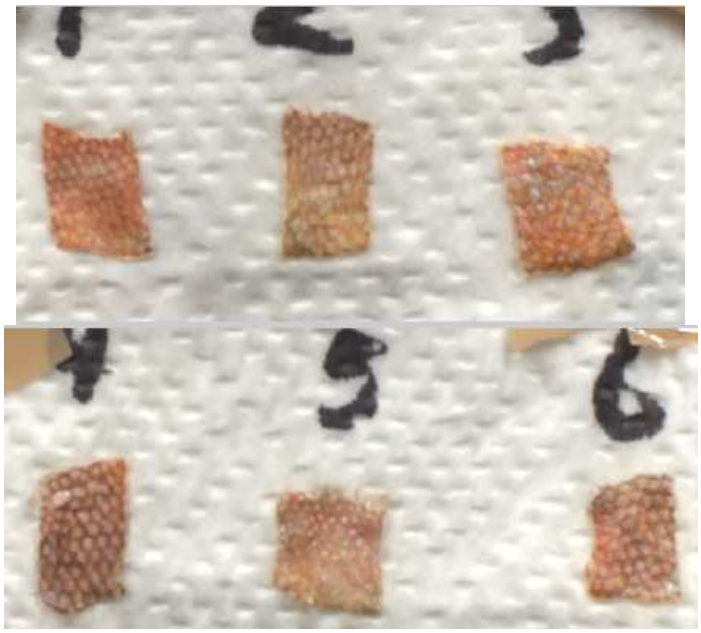

Figure 1: skin samples # 1-6

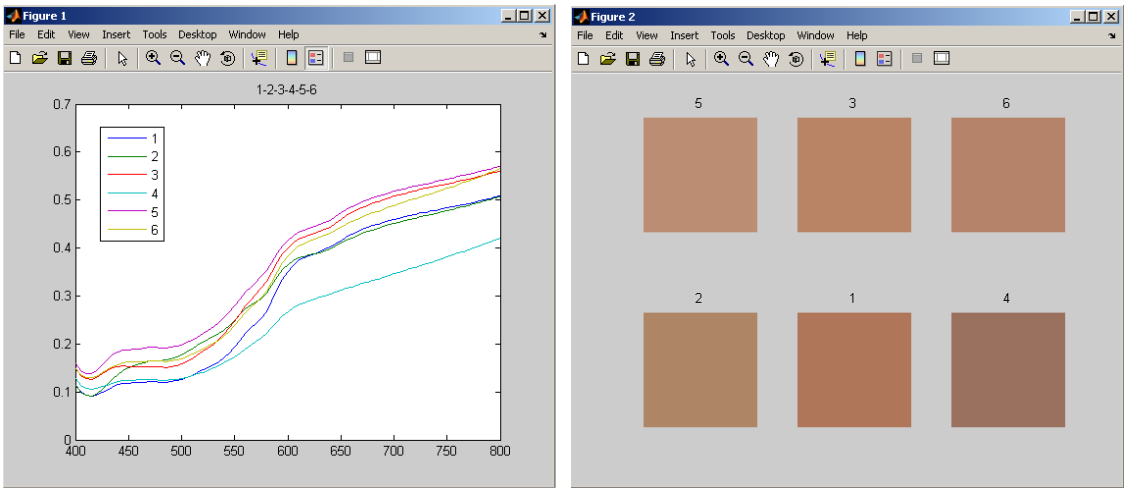

Figure 2: The means of spectral reflectance (on the left) and corresponding color converted in sRGB (on the right)

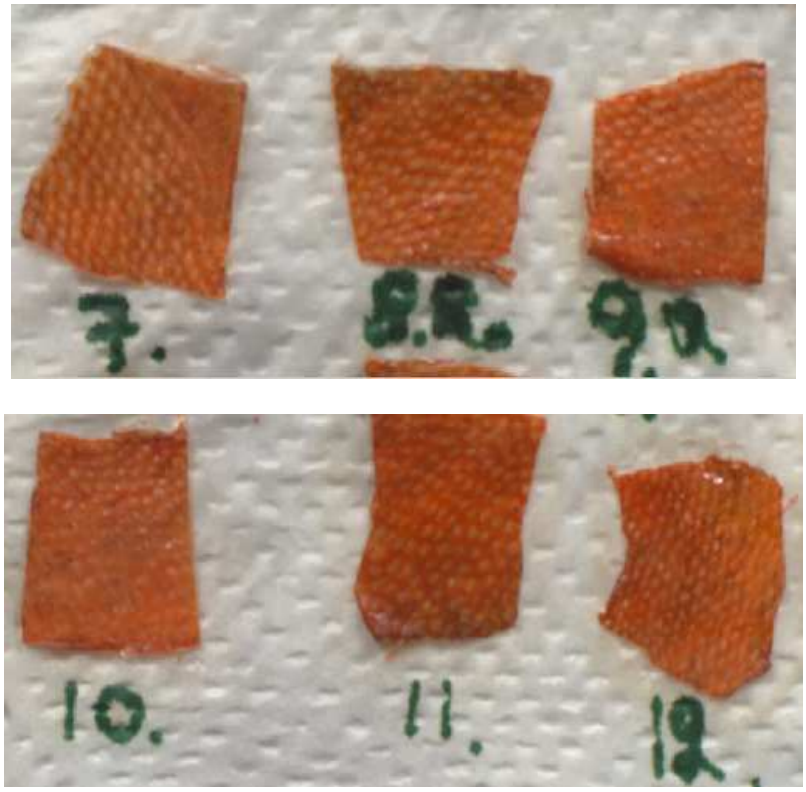

Figure 3: skin samples # 7 – 12

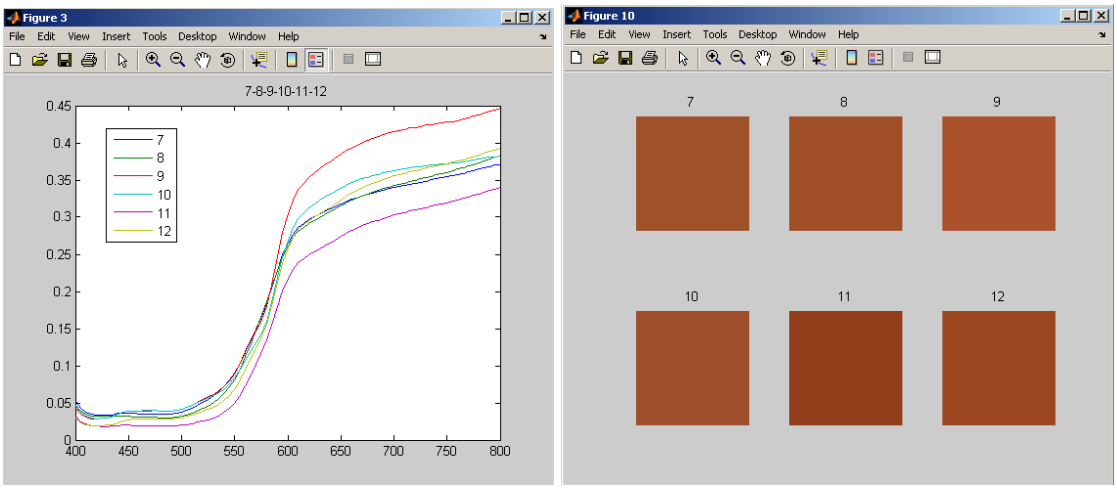

Figure 4: The means of spectral reflectance (on the left) and corresponding color converted in sRGB (on the right)

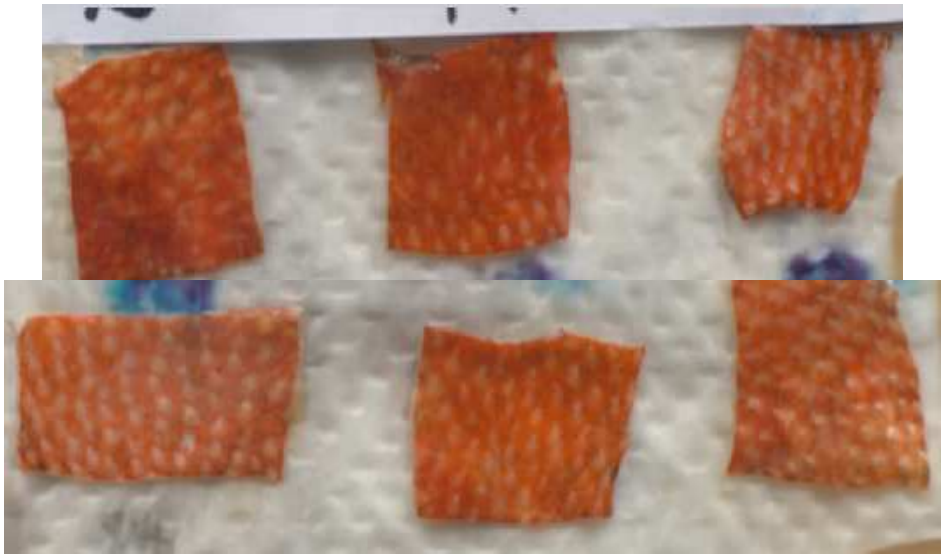

Figure 5: skin samples # 13 – 18

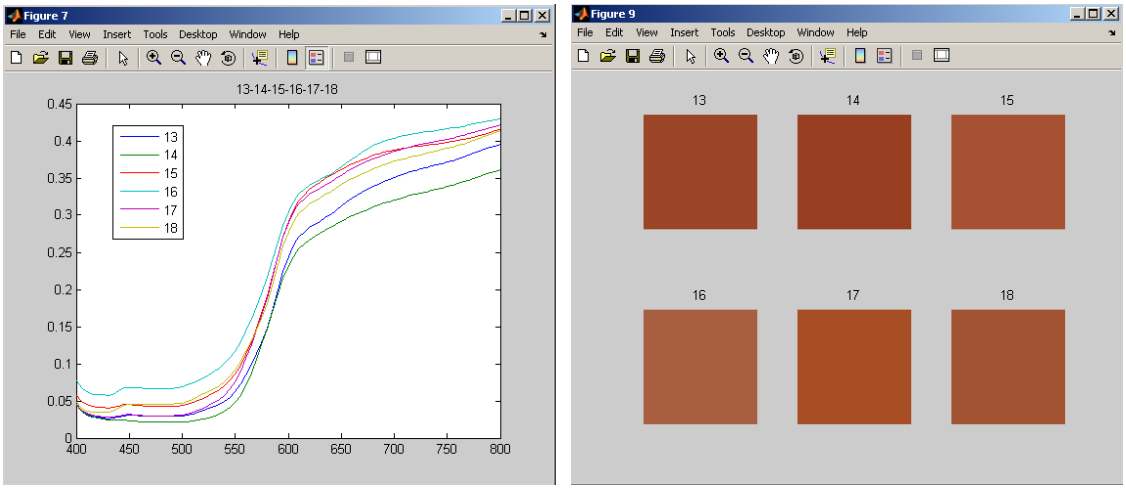

Figure 6: The means of spectral reflectance (on the left) and corresponding color converted in sRGB (on the right)

‘spm.mat’ is matrix with mean of 18 samples

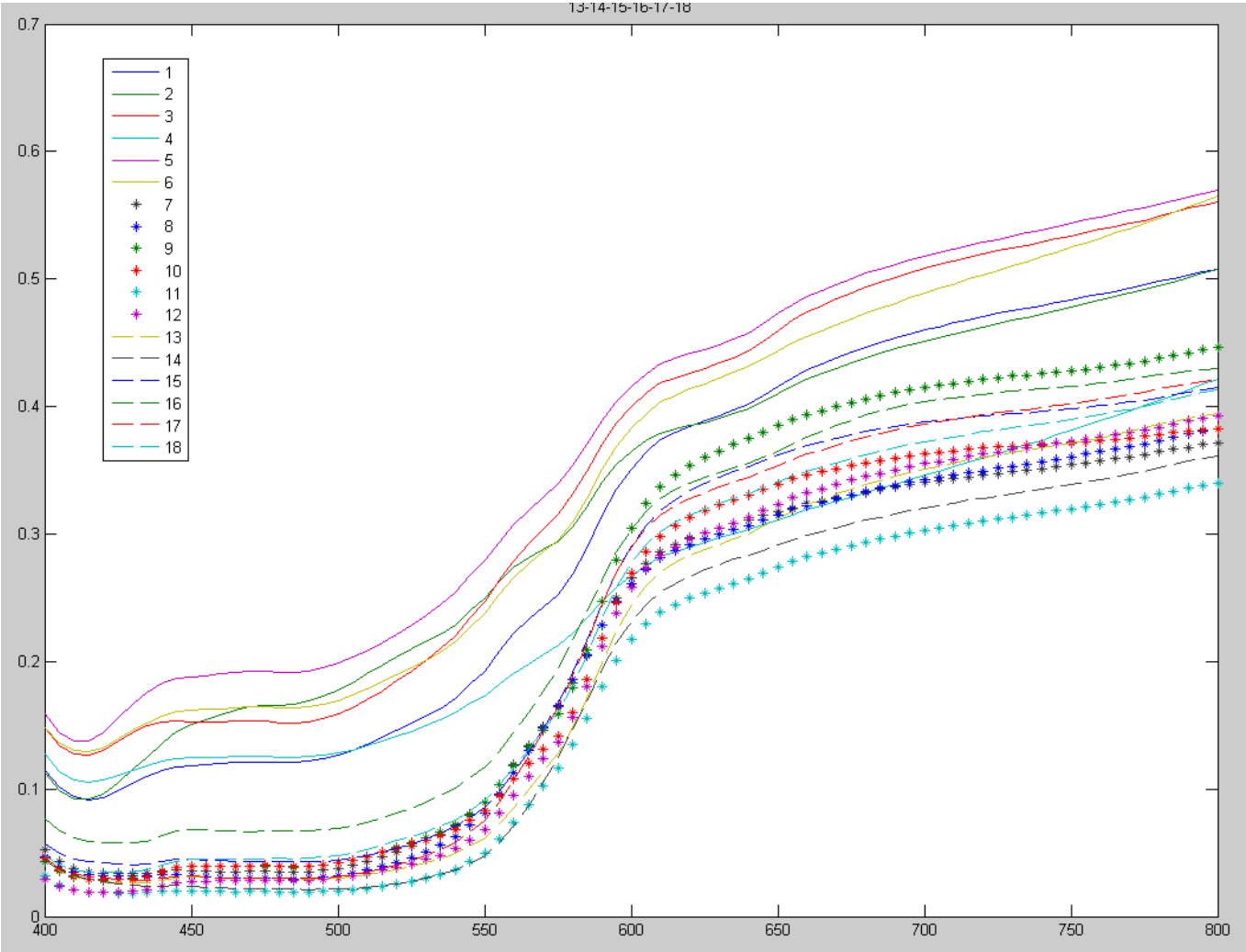

Figure 7: The means of spectral reflectance (samples # 1-18)

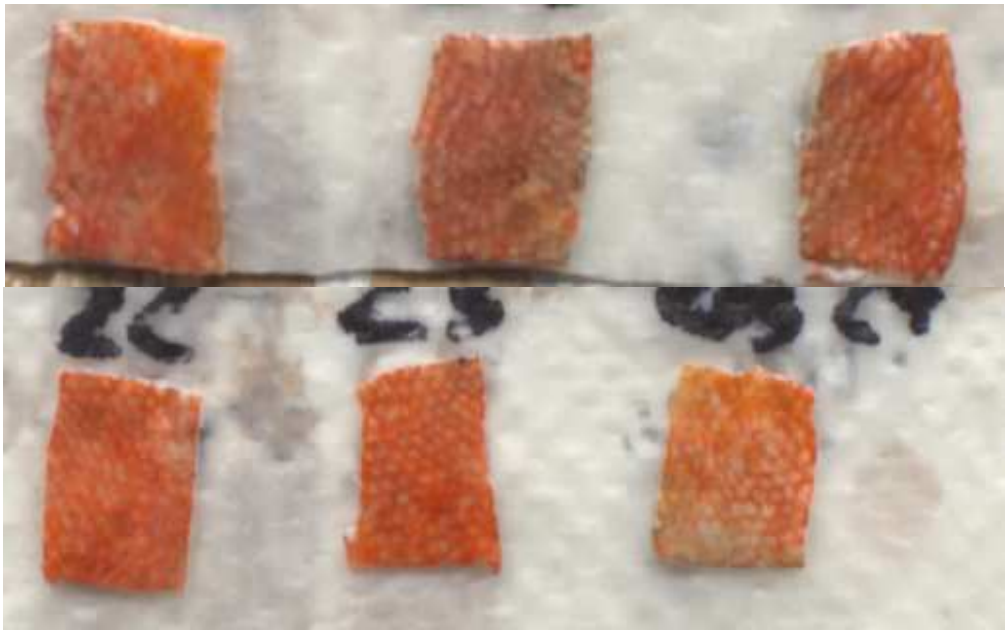

Figure 7: skin samples # 19 – 24

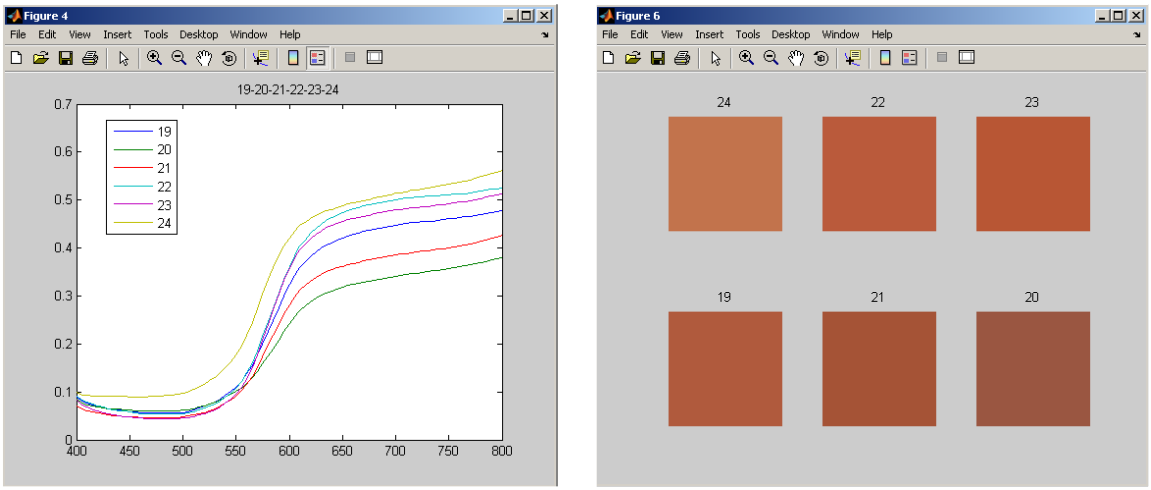

Figure 8: The means of spectral reflectance (on the left) and corresponding color converted in sRGB (on the right)

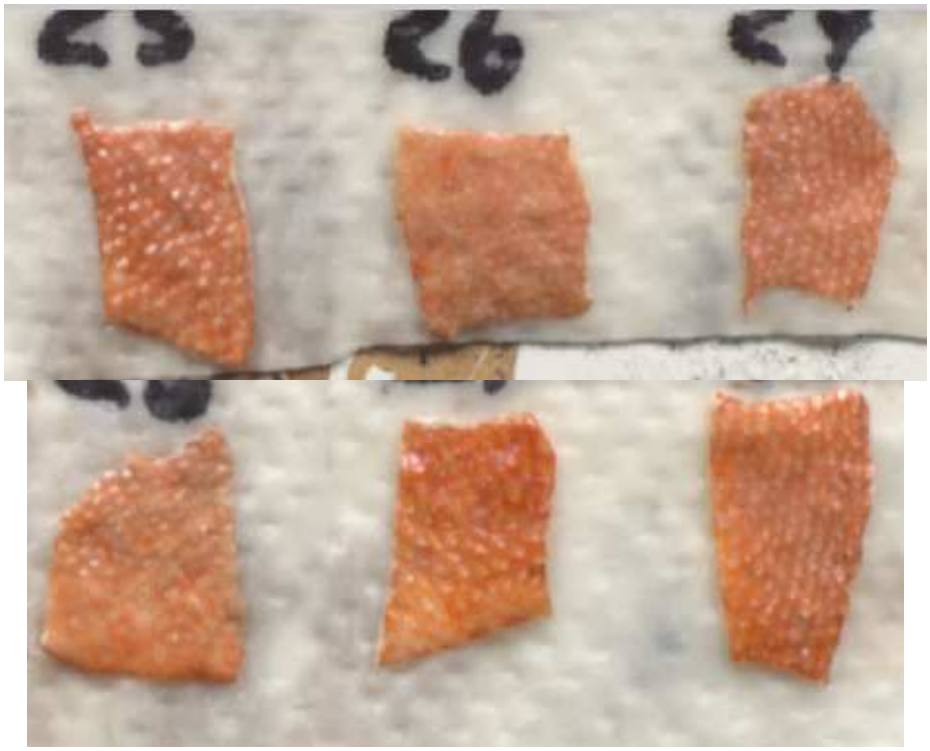

Figure 9: skin samples # 25 – 30

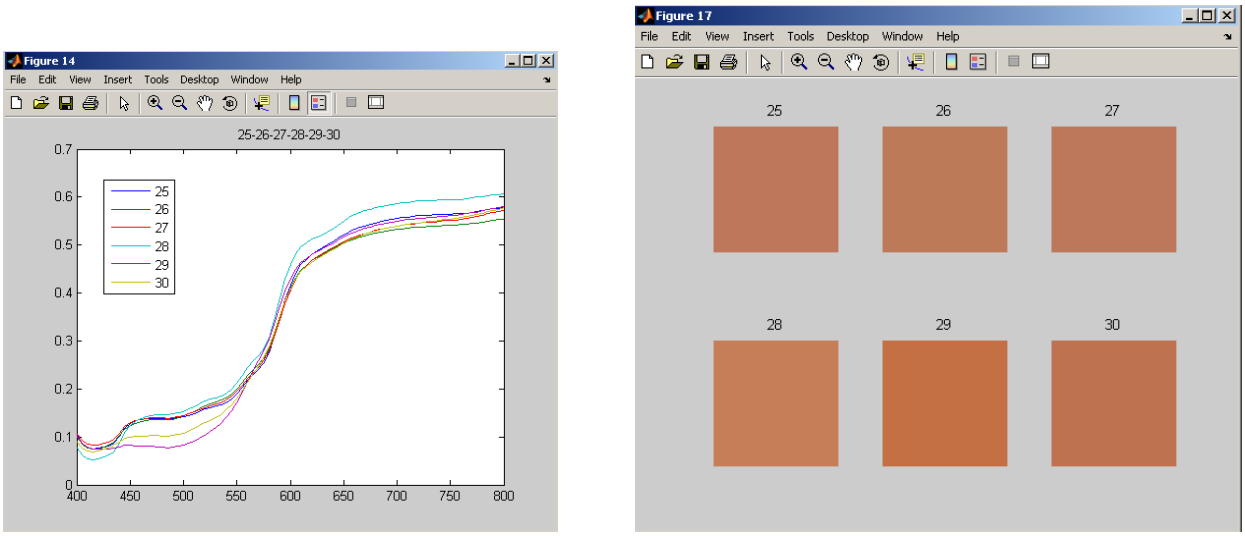

Figure 10: The means of spectral reflectance (on the left) and corresponding color converted in sRGB (on the right)

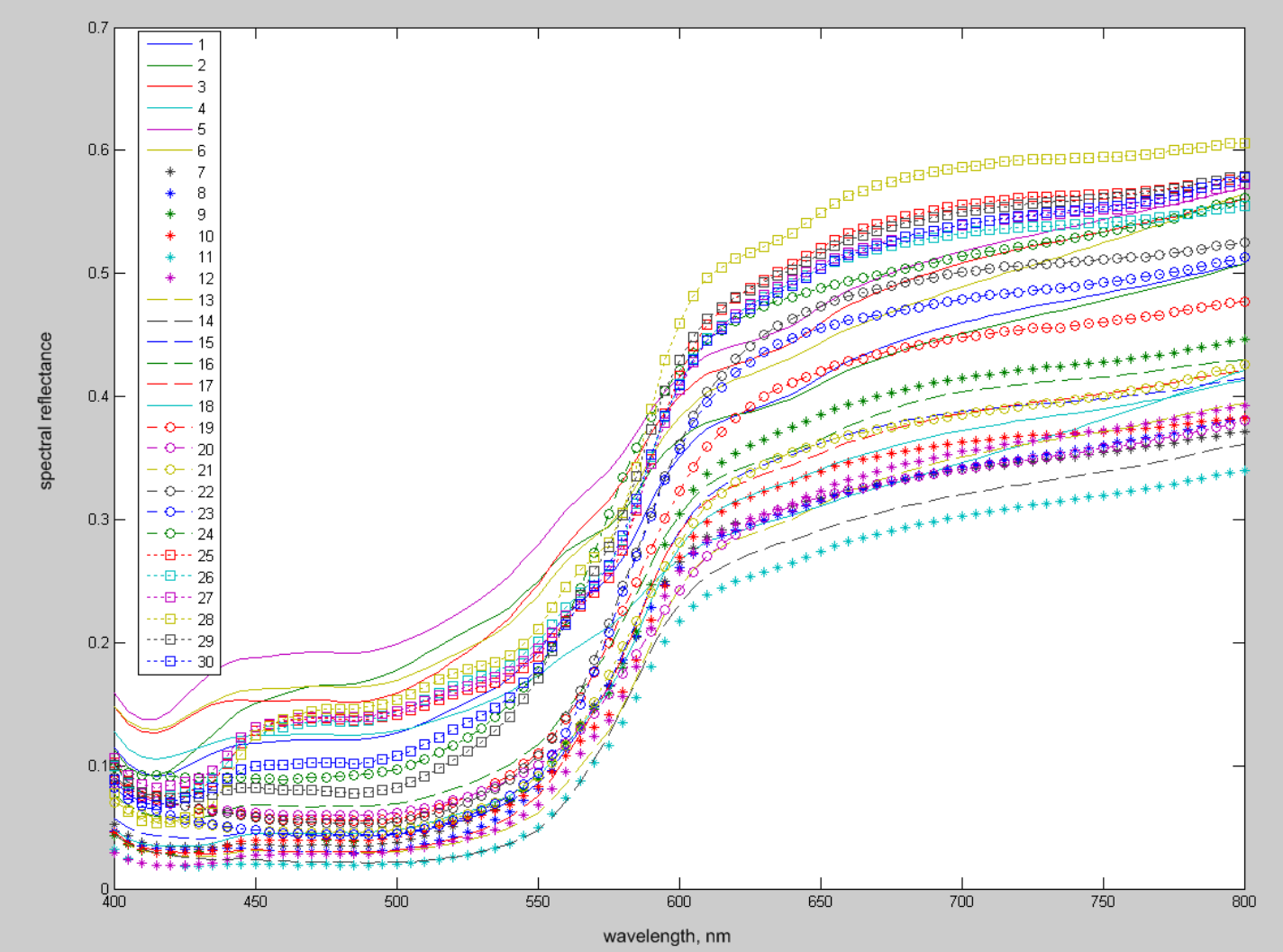

Figure 11: The means of spectral reflectance for skin samples # 1-30 of frozen fish

FRESH FISH SAMPLES

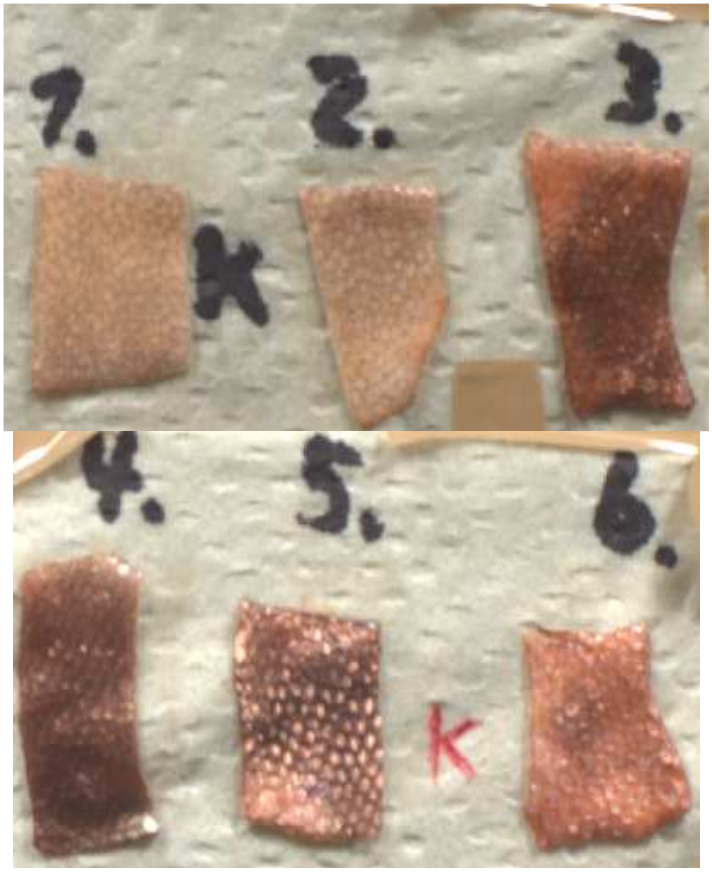

Figure 12: skin samples # 1 – 6

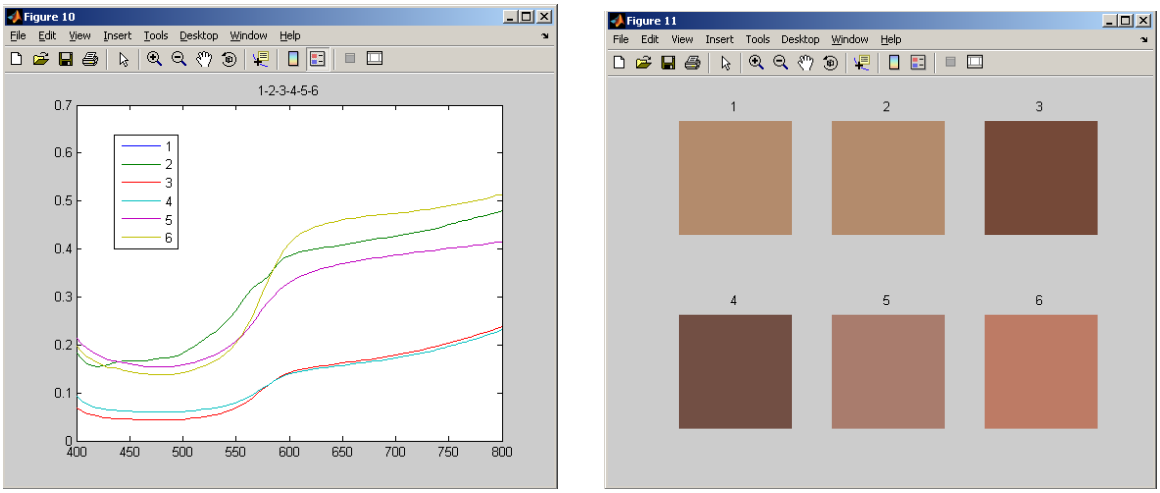

Figure 13: The means of spectral reflectance (on the left) and corresponding color converted in sRGB (on the right)

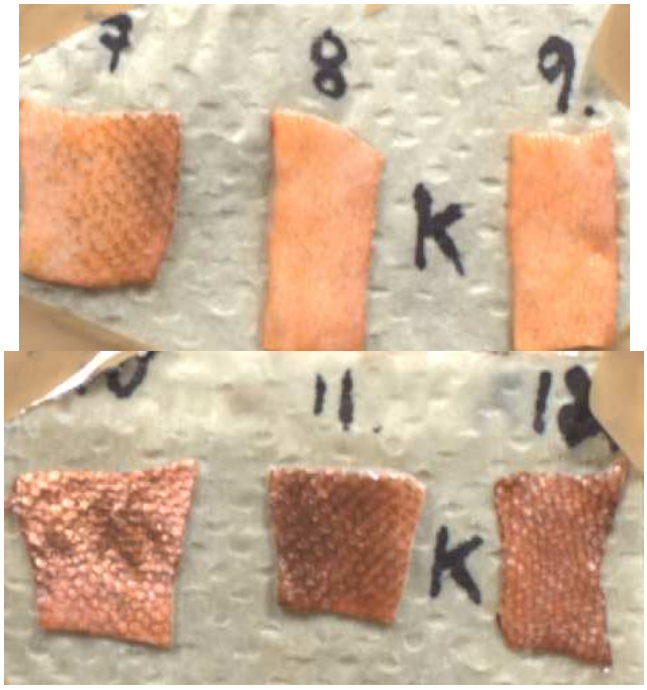

Figure 14: skin samples # 7 – 12

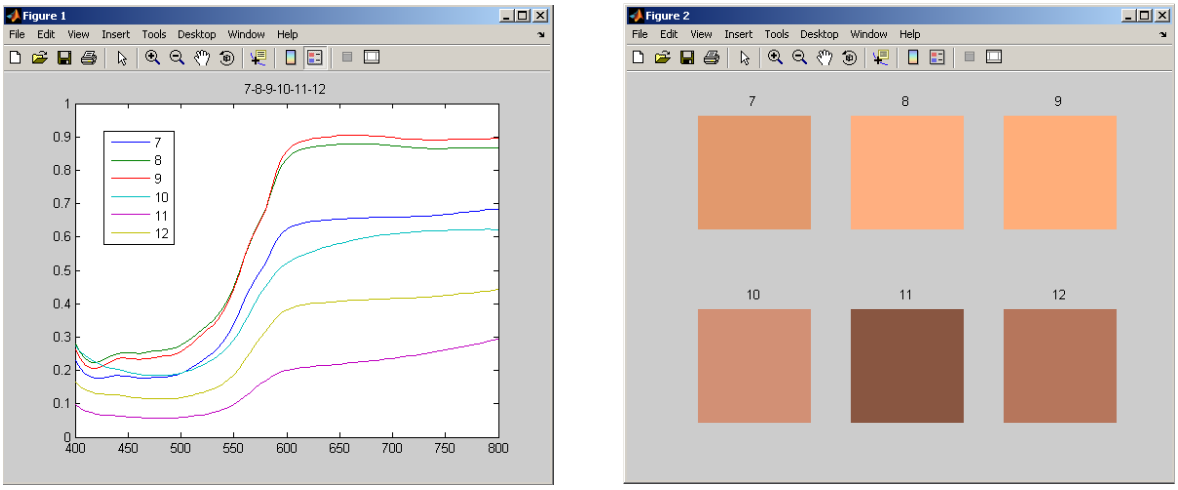

Figure 15: The means of spectral reflectance (on the left) and corresponding color converted in sRGB (on the right)

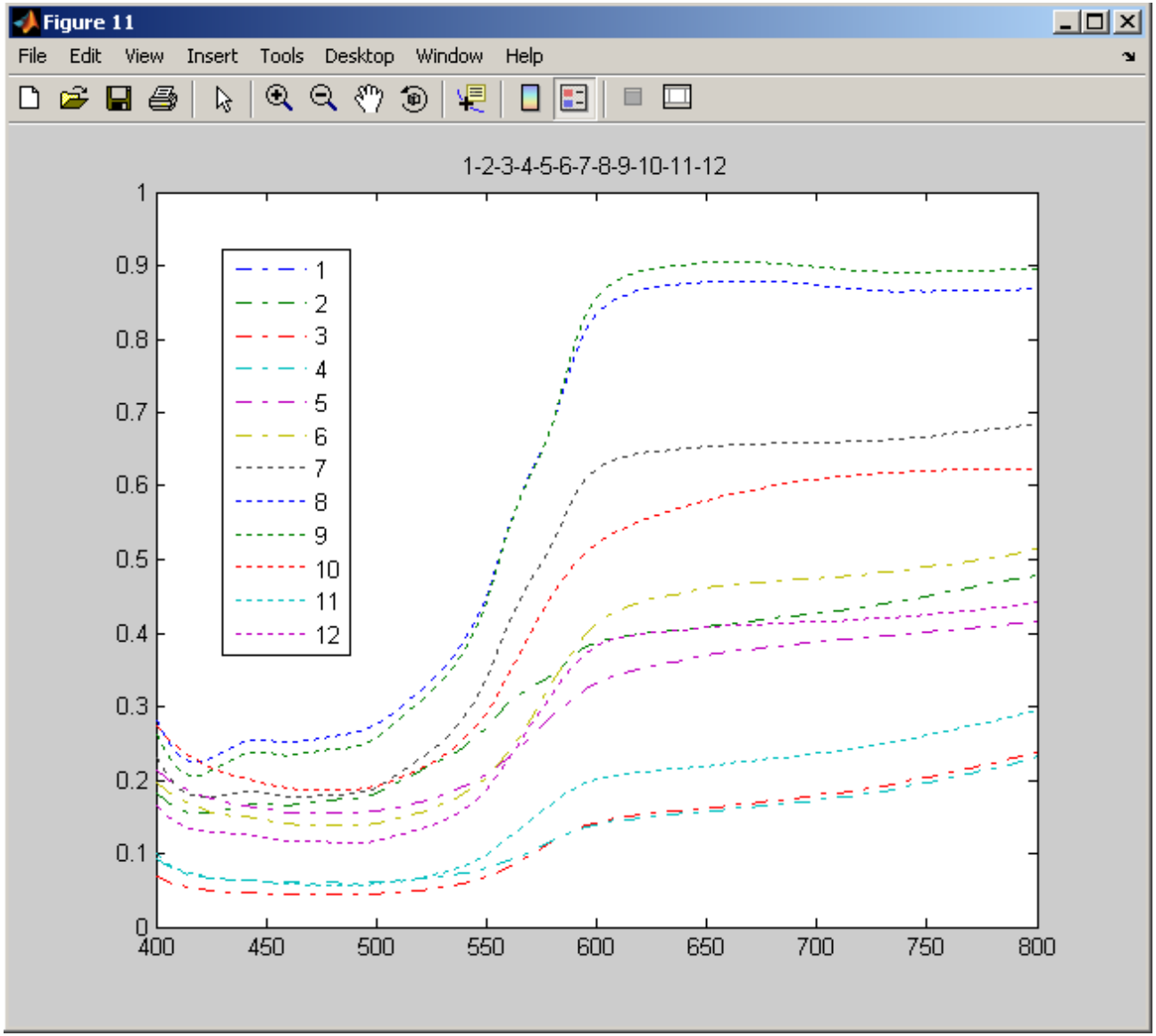

Figure 16: The means of spectral reflectance for skin samples # 1-12 of fresh fish

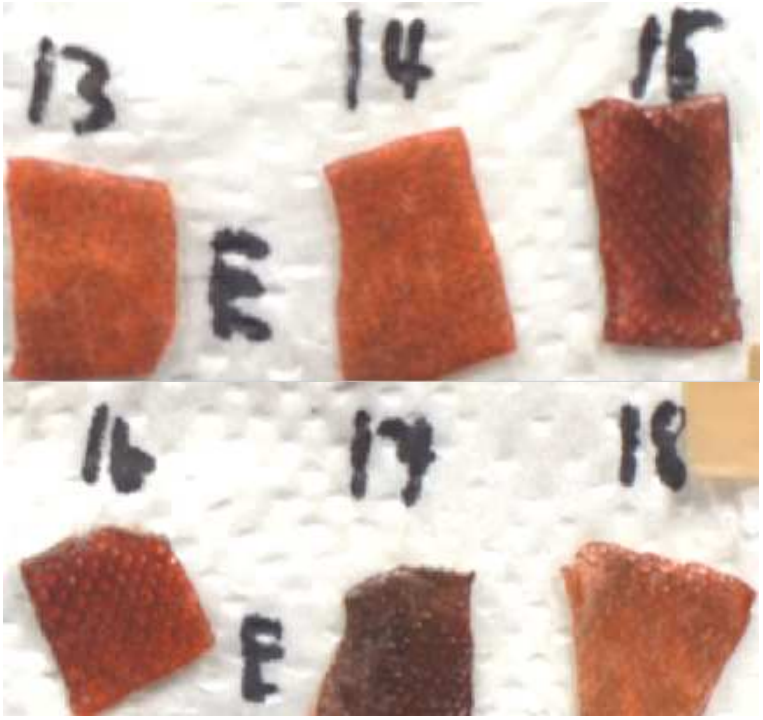

Figure 17: skin samples # 13 – 18

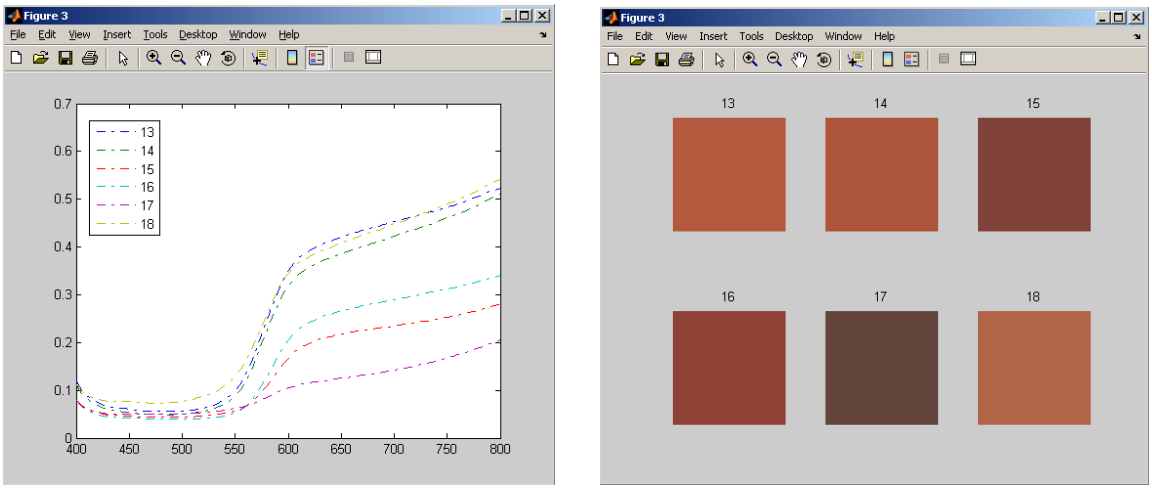

Figure 18: The means of spectral reflectance (on the left) and corresponding color converted in sRGB (on the right)

Figure 19: skin samples # 19 – 24

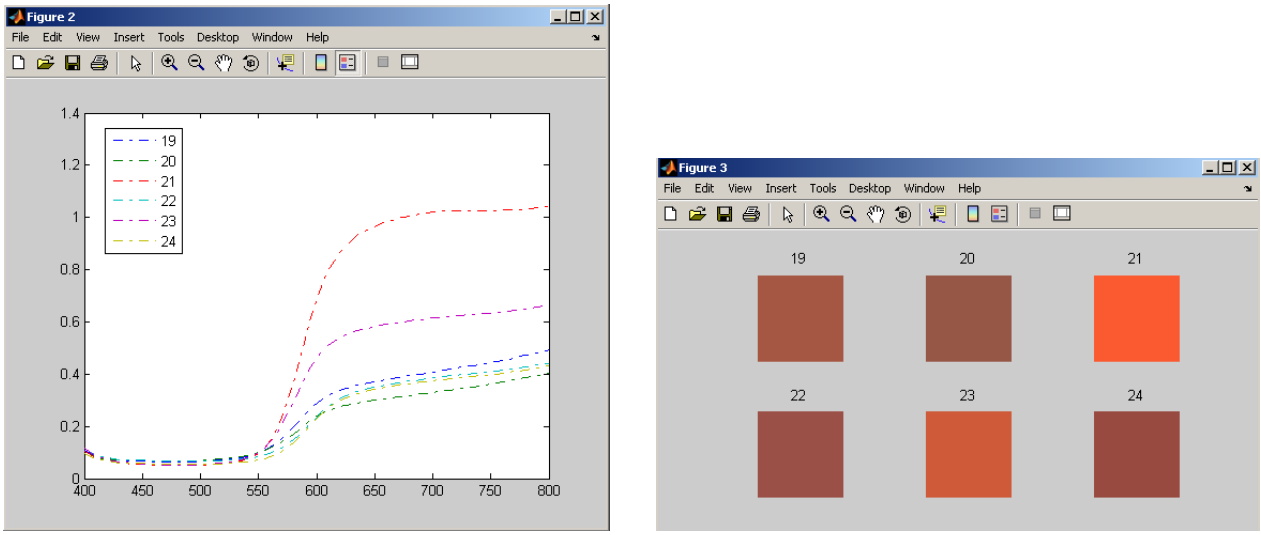

Figure 20: The means of spectral reflectance (on the left) and corresponding color converted in sRGB (on the right)

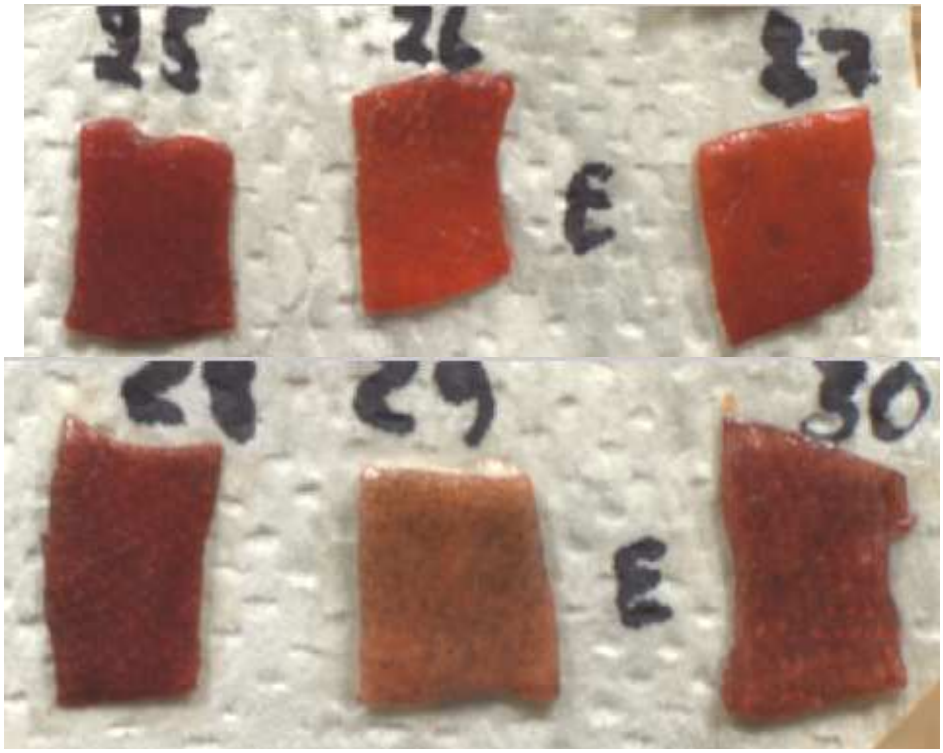

Figure 21: skin samples # 25 – 30

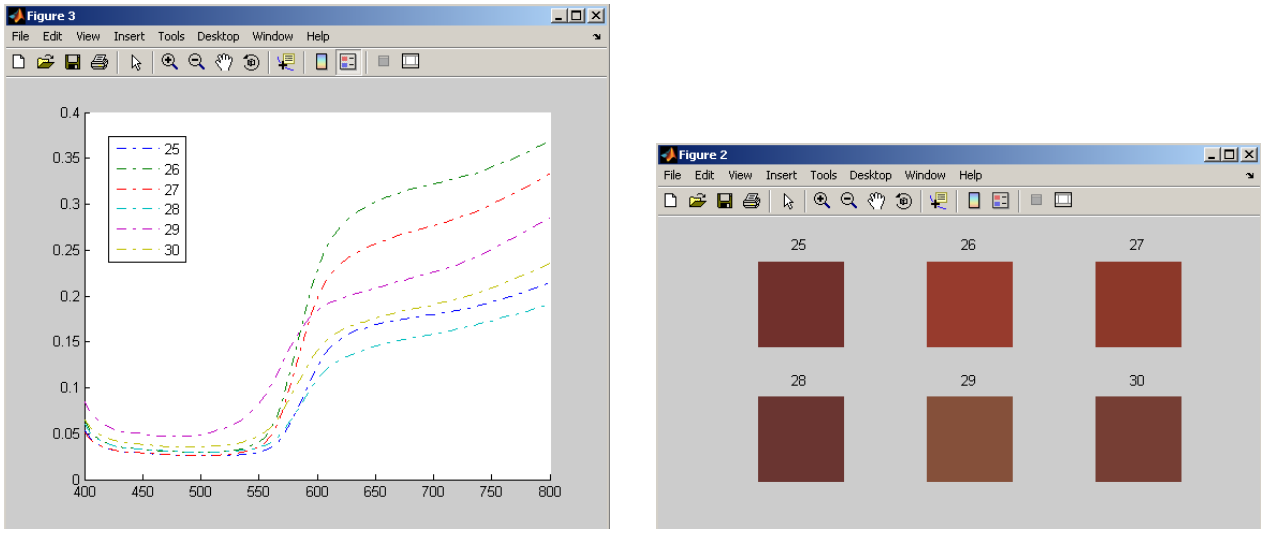

Figure 22: The means of spectral reflectance (on the left) and corresponding color converted in sRGB (on the right)

Figure 23: skin samples # 31 – 36

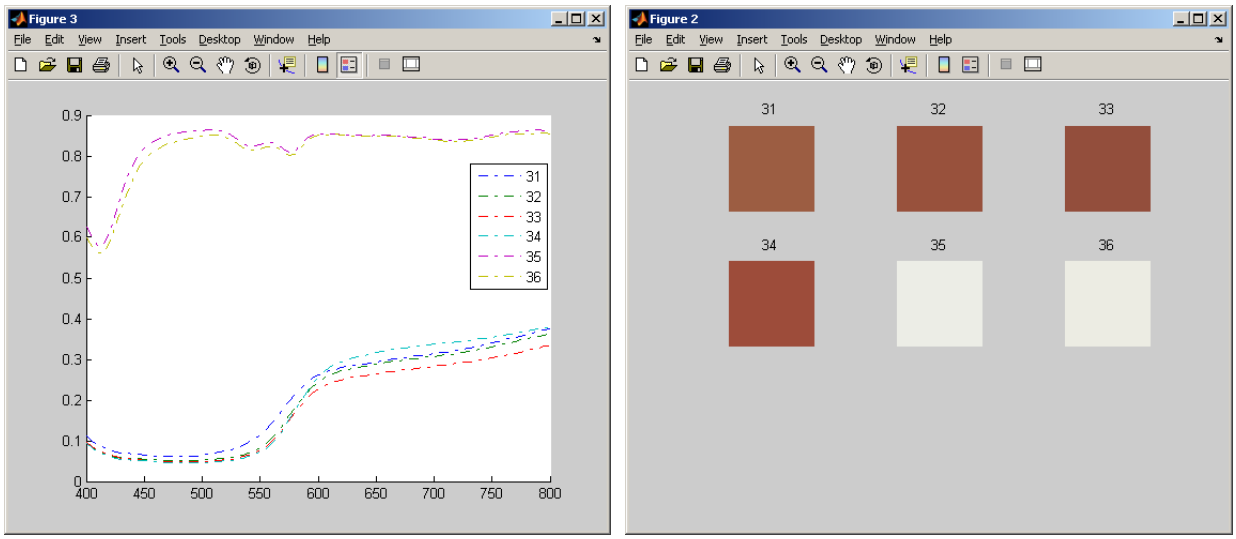

Figure 24: The means of spectral reflectance (on the left) and corresponding color converted in sRGB (on the right)

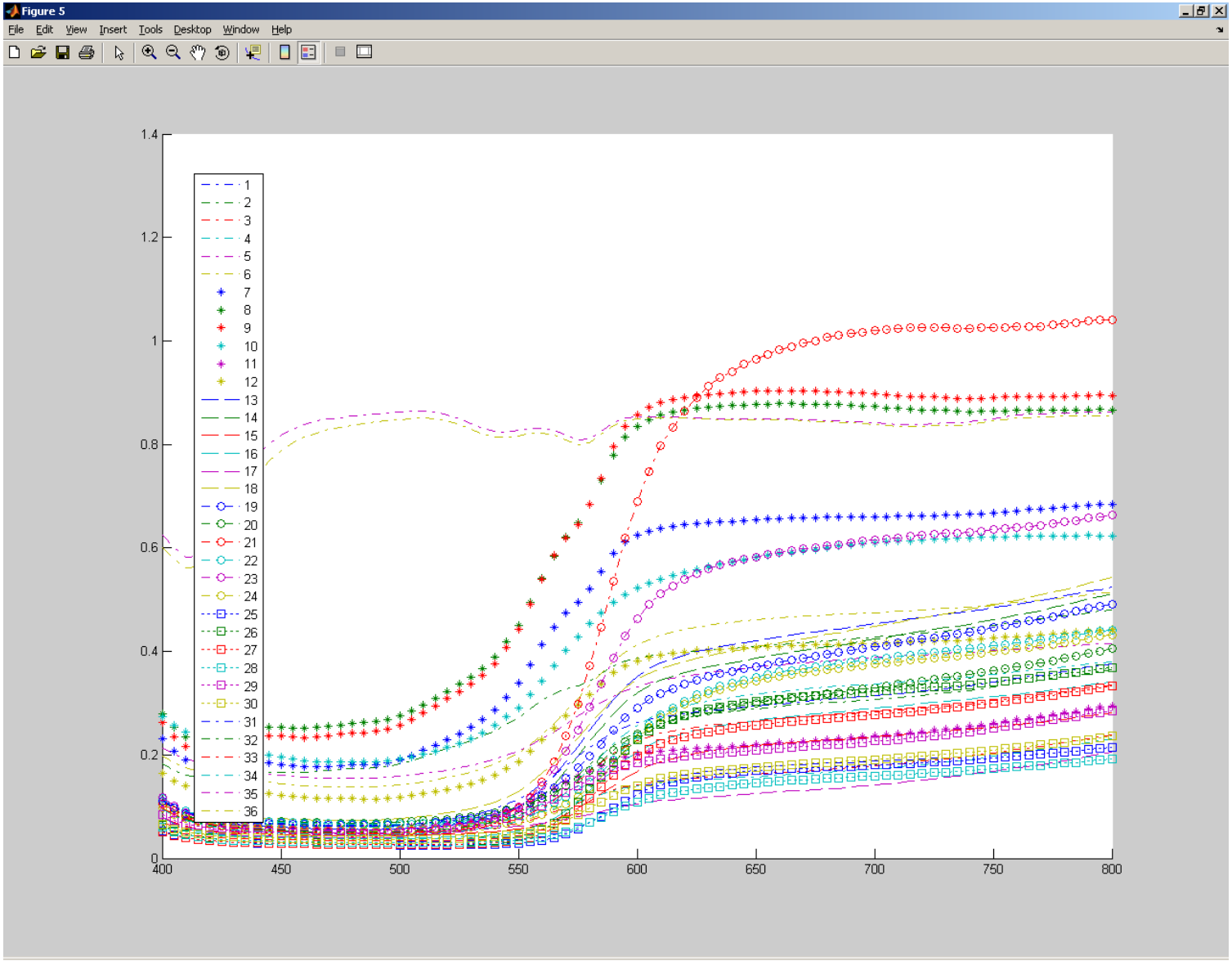

Figure 25: The means of spectral reflectance for samples # 1-36 of fresh fish

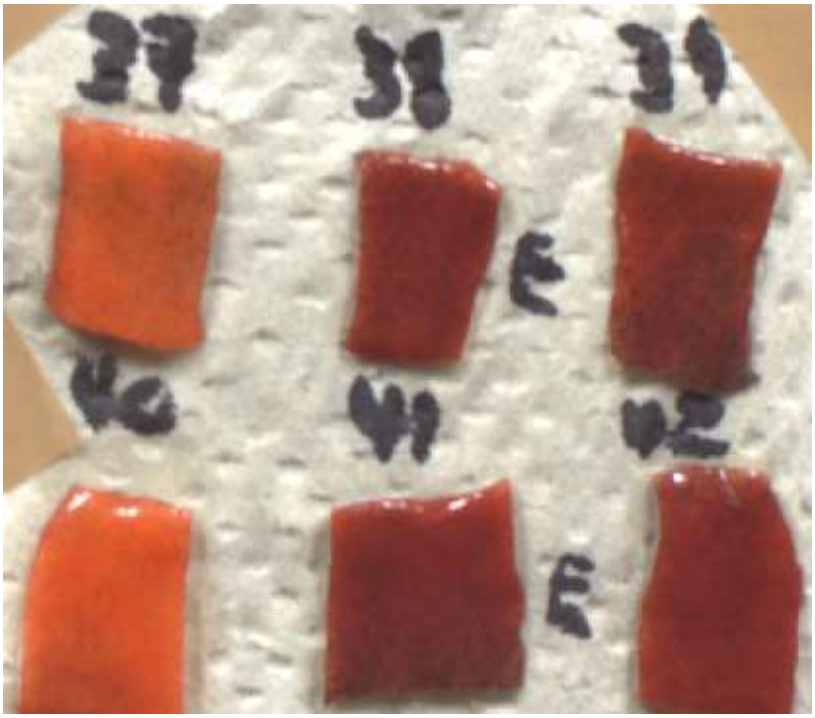

Figure 26: skin samples # 31 – 36

APPENDIX 2: Carotenoid-indices and astraxanthin concentration measured in the skin of Arctic charr

Table 1: Frozen fish

# sample	carotenoid-index R800/R470	astaxanthin µg/g
2	3.09	34.47
5	2.96	40.48
3	3.65	43.74
29	7.24	63.17
6	3.44	65.22
4	3.36	72.88
1	4.19	80.14
25	4.18	85.06
28	4.20	87.40
18	9.18	100.96
14	16.66	103.81
24	6.24	110.04
19	8.56	110.49
30	5.64	115.07
17	13.97	119.47
26	4.08	127.09
20	6.38	133.71
16	6.43	137.56
9	11.31	141.62
27	4.11	144.92
15	9.71	148.95
10	9.60	152.31
7	10.50	156.23
22	9.76	170.98
21	9.27	195.86
23	11.57	199.80
13	13.20	208.32
12	13.87	231.87
11	17.42	242.87
8	12.57	246.16

Table 2: Fresh fish

# sample	carotenoid-index R800/R470	astaxanthin µg/g
35	1.01	0.84
36	1.03	2.88
2	2.84	18.10
1	2.84	22.42
29	6.06	29.26
8	3.40	33.50
11	5.10	36.26
34	8.10	40.35
9	3.78	42.39
31	6.07	43.51
7	3.84	44.56
37	12.06	48.60
33	6.90	53.40
32	7.06	57.69
42	9.80	74.35
41	8.62	76.34
14	10.25	77.72
18	7.37	79.52
12	3.81	81.92
10	3.34	84.66
3	5.48	88.85
13	9.27	97.71
26	11.84	102.05
6	3.70	104.60
30	6.54	105.85
39	8.24	107.62
4	3.84	113.65
27	12.24	122.71
38	9.14	124.84
16	8.42	131.94
19	7.69	135.34
23	12.60	141.28